

Geological Society of America Bulletin

The Akato Tagh bend along the Altyn Tagh fault, northwest Tibet 2: Active deformation and the importance of transpression and strain hardening within the Altyn Tagh system

Eric Cowgill, J Ramón Arrowsmith, An Yin, Wang Xiaofeng and Chen Zhengle

Geological Society of America Bulletin 2004;116, no. 11-12;1443-1464
doi: 10.1130/B25360.1

Email alerting services

click www.gsapubs.org/cgi/alerts to receive free e-mail alerts when new articles cite this article

Subscribe

click www.gsapubs.org/subscriptions/ to subscribe to Geological Society of America Bulletin

Permission request

click <http://www.geosociety.org/pubs/copyrt.htm#gsa> to contact GSA

Copyright not claimed on content prepared wholly by U.S. government employees within scope of their employment. Individual scientists are hereby granted permission, without fees or further requests to GSA, to use a single figure, a single table, and/or a brief paragraph of text in subsequent works and to make unlimited copies of items in GSA's journals for noncommercial use in classrooms to further education and science. This file may not be posted to any Web site, but authors may post the abstracts only of their articles on their own or their organization's Web site providing the posting includes a reference to the article's full citation. GSA provides this and other forums for the presentation of diverse opinions and positions by scientists worldwide, regardless of their race, citizenship, gender, religion, or political viewpoint. Opinions presented in this publication do not reflect official positions of the Society.

Notes

The Akato Tagh bend along the Altyn Tagh fault, northwest Tibet 2: Active deformation and the importance of transpression and strain hardening within the Altyn Tagh system

Eric Cowgill[†]

Department of Earth and Space Sciences, University of California, Los Angeles, California 90095, USA

J Ramón Arrowsmith

Department of Geological Sciences, Arizona State University, Tempe, Arizona 85287, USA

An Yin

Department of Earth and Space Sciences, University of California, Los Angeles, California 90095, USA

Wang Xiaofeng

Chen Zhengle

Institute of Geomechanics, Chinese Academy of Geological Sciences, Beijing, China

ABSTRACT

We investigated active deformation within the Akato Tagh restraining double bend to determine the age of the active Altyn Tagh fault relative to the Altyn Tagh system and thereby evaluate the extent to which this system evolved by net strain-hardening or softening. Active structures were mapped based on their geomorphology and disruption of Quaternary(?) deposits/surfaces. The style of active faulting is strongly correlated with fault strike: 065°–070° striking segments show pure left-slip whereas faults with more northward or eastward strikes are transtensional or transpressional, respectively. Our mapping further suggests that the 065° to 070°-striking western and eastern segments of the Akato Tagh bend are characterized by pure strike-slip motion, with partitioned transpression along the ~090°-striking central segment of the double bend. It remains unclear how this active, bend-perpendicular shortening is absorbed. In conjunction with previous work, the present study fails to support the commonly held idea that Tarim-Tibet motion is strongly oblique to the Altyn Tagh system. Estimates for the age of the Akato Tagh bend derived in a companion study suggest the bend is only a few million years old. The current principal trace is

probably similarly young because formation of the bend by recent deformation of an old trace should result in transpression along the western and eastern segments, contrary to the pure left-slip shown here. The Altyn Tagh system comprises multiple fault strands in a zone ~100 km wide across strike. Because the main trace appears to be much younger than the system in which it is embedded, we speculate that this system evolved by the sequential formation and death of short-lived fault strands. In particular, we suggest that geometrically complex strike-slip fault systems such as the Altyn Tagh may form via system strain hardening, where this net response reflects a dynamic competition between hardening and softening processes that are active simultaneously within the fault zone. Hardening mechanisms may include growth of restraining bend topography or material hardening of phyllosilicate-rich gouge, whereas softening processes might include R-P shear linkage or reduction in bend angle by vertical axis rotation. Our analysis suggests that net strain hardening of a fault system can produce continental deformation that is spatially localized over the 1–5 m.y. during which an individual strand is active, but distributed over the 10–100 m.y. corresponding to the life-span of the whole fault system and the collision zone in which it is contained. Thus, time scale is critically important in determining whether or not continental deformation is spatially distributed or localized.

Keywords: strike-slip systems, restraining double bends, Altyn Tagh fault, transpression, strain hardening, active faulting.

INTRODUCTION

The Himalayan-Tibetan orogen is the largest active zone of continental collision on Earth and thus provides an excellent opportunity to better understand the deformational behavior of the continental lithosphere. Kinematic models of the orogen (e.g., Avouac and Tapponnier, 1993; England and Molnar, 1997; Holt, 2000; Holt et al., 2000; Kong and Bird, 1996; Peltzer and Saucier, 1996) suggest that over short time scales (10^4 to 10^6 years) most deformation is localized along a few major fault systems that separate effectively rigid blocks or microplates. However, it is not clear if such a description remains accurate at longer time scales (10^7 to 10^8 years). According to one view, long-term deformation is localized along major fault systems, and thus mimics the pattern seen at short time scales (e.g., Peltzer and Tapponnier, 1988; Tapponnier et al., 2001). An alternative view holds that long-term deformation is broadly distributed (e.g., England and Houseman, 1986; Houseman and England, 1996).

One of the most striking aspects of the Indo-Asian collision zone is that it is cut by a number of strike-slip fault zones that approach the size of plate boundaries (Fig. 1) (Molnar and Tapponnier, 1975; Tapponnier and Molnar, 1977). According to the lateral extrusion model (e.g., Molnar and Tapponnier, 1975; Peltzer and

[†]Present address: Department of Geology, University of California, Davis, California 95616, USA; e-mail: cowgill@geology.ucdavis.edu.

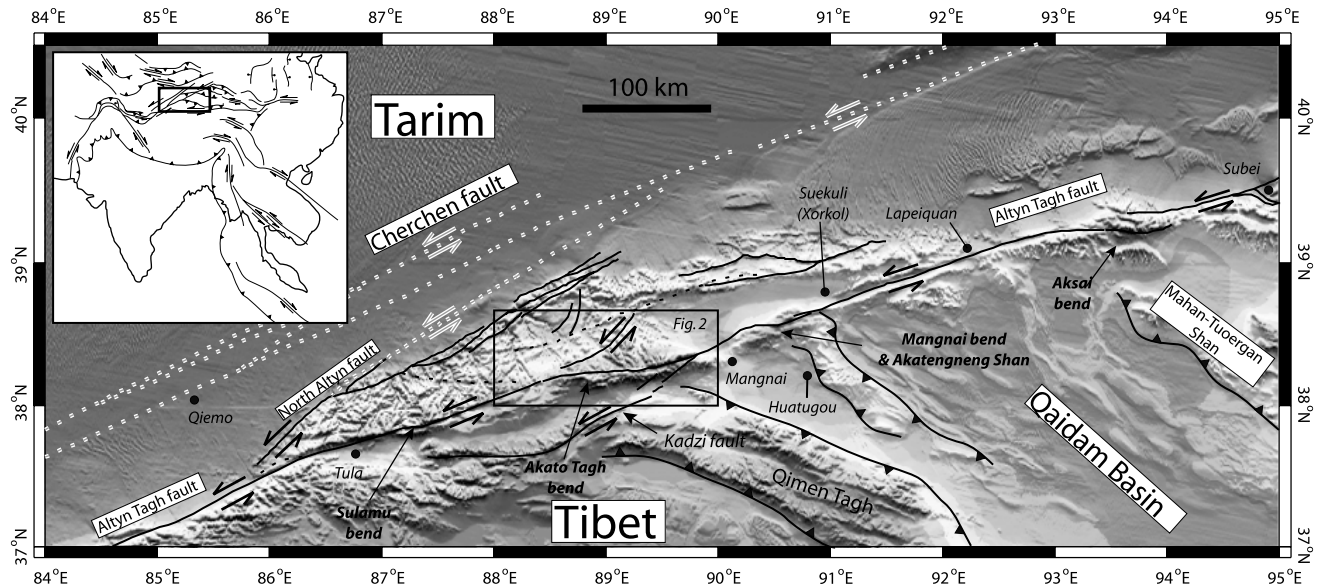


Figure 1. Shaded relief image of the central Altyn Tagh range showing known and inferred Cenozoic faults within the Altyn Tagh system. Inset shows the major structures within the Indo-Asian collision zone (box outlines location of Fig. 1). Faults were compiled from our mapping and interpretation of stereo CORONA satellite imagery as well as previous investigations (Chinese State Bureau of Seismology, 1992; Cowgill et al., 2000; Liu, 1988; Meyer et al., 1998). The Sulamu Tagh, Akato Tagh, Akatengneng Shan, and Aksai uplifts are centered on restraining double bends along the Altyn Tagh fault. Each bend is located along strike from a thrust belt to the south of the main trace. Box in main figure shows location of Figure 2. Base map was generated from the GTOPO30 1 km digital elevation data using GMT software developed by Wessel and Smith (1991).

Tappouer, 1988; Tappouer et al., 2001), these strike-slip systems are lithospheric-scale structures that have accommodated Indo-Eurasian convergence by allowing east-directed horizontal expulsion of lithospheric blocks out of the path of the Indian indenter. A fundamental requirement of the lateral-extrusion hypothesis is that these faults evolve by strain-softening: as deformation progresses, strain within incipient strike-slip shear zones becomes localized as fault strength decreases to produce long-lived (10+ m.y.), fast-moving (10+ mm/yr) faults with large magnitudes of total displacement (100+ km). However, major intracontinental strike-slip systems typically have strike-perpendicular widths of 100 km or more. If the width of these zones increases during progressive deformation, then an alternative possibility is that they evolve by net strain-hardening at time scales of 10⁷ to 10⁸ years. Distinguishing between these two scenarios in the case of the Himalayan-Tibetan orogen requires determining the age and structural evolution of the major strike-slip systems within the collision zone. In particular, have these major strike-slip systems evolved from distributed to localized zones of faulting, suggesting strain softening, or have they developed by the sequential formation and abandonment of individual strands, implying strain hardening?

The active, left-lateral Altyn Tagh fault system (Fig. 1) (Molnar and Tappouer, 1975, 1978; Tappouer and Molnar, 1977) is the largest strike-slip system in Asia. The Altyn Tagh system comprises a broad zone of generally northeast-striking faults separating the Tarim basin to the north from the Qaidam basin and Tibetan Plateau to the south (Fig. 1). In contrast to this broad zone of finite strain, active deformation appears to be concentrated along the principal active trace, the Altyn Tagh fault. The latter structure is well expressed geomorphically, and is punctuated by a set of four, right-stepping restraining double bends between 85°E and 95°E longitude (Fig. 1), the largest of which coincides with the 90-km long Akato Tagh range. Within the Akato Tagh bend, the Altyn Tagh fault comprises three segments, with an east-west striking central segment that is flanked by 060–070° striking faults to the west and east (Fig. 2).¹ Where these segments intersect they create “inside corners” within the southwestern and northeastern sectors of the Akato Tagh (Fig. 2 inset).

To investigate the age of the active trace of the Altyn Tagh fault relative to the Altyn Tagh system as a whole, we have studied both the active and bedrock deformation within the Akato Tagh

range. A companion study (Cowgill et al., 2004) emphasizes the relationship between the topography of the Akato Tagh range and the underlying bedrock structure. Cowgill et al. (2004) investigates the long-term deformation field around the Akato Tagh double bend and similar jogs along other major strike-slip faults to determine how such geometric complexities evolve. That study suggests that the bend is probably only a few million years old, much younger than the Altyn Tagh system. The bedrock geology described in Cowgill et al. (2004) records finite strain that has likely accumulated over at least several million years. Here we address two questions regarding the neotectonics of the bend: (1) Is transpression restricted to the central segment of the restraining bend, or does it also occur along the western and eastern fault segments, and (2) to what extent does the pattern of active deformation mimic the longer-term record? To address these questions we have mapped active deformation within and adjacent to the Akato Tagh bend. Our approach investigates deformation at a regional scale (~1:100,000) using CORONA satellite image analysis and field observations, a local scale (~1:60,000) using field observations and air photo interpretation, and a detailed scale (~1:5000) using field surveys.

After reviewing the regional structural setting of the Altyn Tagh fault, we summarize

¹Figure 2 is on a separate sheet accompanying this issue.

the basic Quaternary stratigraphy within the Akato Tagh bend, and then describe the active deformation proceeding from west to east. We then integrate our results with previous work to evaluate the extent to which the Altyn Tagh fault is a transpressional plate boundary that shows strain-hardening behavior.

STRUCTURAL FRAMEWORK OF CENTRAL ALTYN TAGH FAULT

Altyn Tagh System

The Altyn Tagh fault system lies along the northwest margin of the Tibetan Plateau and extends from the Cherchen fault in the northwest to the Altyn Tagh fault, ~100 km to the southeast (Fig. 1). Additional major strands include the North Altyn, Keruke and Kadzi faults (Fig. 1). The ~600-km-long Altyn Tagh range lies within this system as a tectonic sliver.

The Altyn Tagh Fault

The southern edge of the Altyn Tagh range is defined by the active, left-slip Altyn Tagh fault, the principal active strand. Between 85°E and 95°E longitude, this trace consists of a series of five straight fault sections that are punctuated by four shorter, right-stepping, east-west trending segments. We follow Crowell (1974) in calling such geometric complexities “restraining double bends.” Mountain ranges flank each double bend (Figs. 1B and 2), suggesting they are localized sites of active horizontal shortening.

Early investigations of the Altyn Tagh fault based on Landsat image interpretation and reconnaissance field studies documented left-slip offsets along the active trace (Tapponnier and Molnar, 1977) and the probable recurrence of large-magnitude earthquakes (Molnar et al., 1987a; Molnar et al., 1987b). Subsequent work has concentrated on the initiation age (Rumelhart, 1998; Wang, 1997; Yin et al., 2002; Yue et al., 2001), total offset (Chen et al., 2002; Cowgill et al., 2003; Ritts and Biffi, 2000; Wang, 1997; Yin and Harrison, 2000; Yue et al., 2001; Yue et al., 2004; Zheng, 1991, 1994), paleoseismic history (Chinese State Bureau of Seismology, 1992; Washburn et al., 2000; Washburn et al., 2001; Washburn et al., 2003), and slip rate at different time scales including the late Tertiary (<10 mm/y, Yue et al., 2003), Quaternary (~30 mm/y, Meriaux et al., 1997; Meriaux et al., 2000; Meriaux et al., 1998; Van der Woerd et al., 2001), and active rates (~10 mm/y, Bendick et al., 2000; Shen et al., 2001).

The Altyn Tagh system appears to have initiated by ~49 Ma. By integrating new magnetostratigraphic analyses, detrital fission-track data, and sandstone petrofacies work with existing

biostratigraphic and lithostratigraphic data of Cenozoic basins along the northwestern margin of Tibet, Yin et al. (2002) demonstrated that syntectonic deposition had begun by ~49 Ma within basins along the northwest margin of Tibet. These results constrain the initiation age of the Altyn Tagh system because these basins are controlled by thrust belts that either branch from or terminate the left-slip system. The ~49 Ma initiation age is consistent with apatite fission track data that suggest either Paleocene(?)–Eocene (Sobel et al., 2001) or 40 ± 10 Ma (Jolivet et al., 2001) basement cooling of ranges within or adjacent to the Altyn Tagh fault system, possibly reflecting initiation of Cenozoic left-slip. Cooling histories derived from analysis of $^{40}\text{Ar}/^{39}\text{Ar}$ K-feldspar results in the context of multi-diffusion domain theory are consistent with an ~49 Ma initiation age in that they suggest the system was active by at least mid-Oligocene time (Cowgill et al., 2001).

In contrast to the Middle Eocene initiation age determined by Yin et al. (2002), Yue et al. (2001) used sediment-source reconstructions of Tertiary deposits in the Xorkol basin (Fig. 1) to infer that the Altyn Tagh fault initiated during the latest Oligocene–earliest Miocene and has 375 ± 25 km of total slip. However, this study failed to consider the obvious possibility that large-magnitude, pre-Oligocene left-slip could have occurred along the Altyn Tagh fault without being recorded by the deposits within the Xorkol basin. Thus Yue et al. (2001) have only determined *minimum* estimates for the initiation age and total slip.

North Altyn and Cherchen Faults

The North Altyn fault separates the Altyn Tagh range to the south from the Tarim basin to the north (Fig. 1). Structural mapping and analysis of fault-zone fabrics indicates that a 120-km-long segment of the fault at its western end is dominated by left-slip motion with a subsidiary component of thrusting: measured slip directions trend 045° to 060° along faults that strike 060° and dip 60–70° south. Cowgill et al. (2000) also mapped a small, right-stepping bend along the North Altyn fault. Paleomagnetic data indicate Upper Oligocene strata adjacent to the bend have undergone $10.6^\circ \pm 7.8^\circ$ of counterclockwise rotation (Rumelhart et al., 1999; as corrected in Yin et al., 2000), consistent with their proposed strike-slip translation through the bend along the North Altyn fault.

Quaternary alluvial deposits overlie the North Altyn fault and led Cowgill et al. (2000) to conclude that this structure is either inactive or has a low slip rate. The latter seems more likely considering the sharpness of the range front and recent seismicity with strike-slip focal mechanisms in the vicinity of this structure (Ma, 1980). Several

drainages and bedrock ridges show left separations on CORONA satellite photographs of the Altyn Tagh range front between 87°E and 89°E longitude, along strike to the northeast of the area mapped by Cowgill et al. (2000). Topographic ridges between 91°E, 40°N and 93°E, 41°N lie along strike of the North Altyn fault system, near its intersection with the Cherchen fault (Fig. 1). Previous mapping (Xinjiang Bureau of Geology and Mineral Resources, 1993) indicates these ridges coincide with faults that cut Neogene and Quaternary units, suggesting the North Altyn fault system continues along strike into the Tarim. Figure 1 shows a compilation of these inferred structures as dashed lines. Reconnaissance work along the range front at 38.978°N, 88.725°E indicated limited evidence for low rates of active faulting (Washburn, 2001).

The Cherchen fault (Fig. 1) is a steeply dipping structure that strikes parallel to the Altyn Tagh fault, and extends from 80°E longitude in the western Kunlun Shan to at least 92°E longitude (Jia, 1997; Liu, 1988; Xinjiang Bureau of Geology and Mineral Resources, 1993). The Xinjiang geologic map (Xinjiang Bureau of Geology and Mineral Resources, 1993) shows high-angle faults within the Cherchen system near 40°N, 92°E that strike parallel to the Altyn Tagh fault and cut Paleozoic through Quaternary rocks, including Paleogene–Neogene units. The map also shows ~10 km of left separation of a contact between Quaternary and Carboniferous units. Although seismic sections indicate the fault cuts Miocene rocks, it shows minimal vertical separation of Tertiary units (Kang, 1996). Linear ridges continue along strike of the Cherchen and North Altyn faults to the east of 92°E longitude within the Tarim basin (Fig. 1) and appear to link with a set of left-lateral strike-slip faults that lie farther along strike to the northeast within Mongolia (Lamb and Badarch, 1997; Lamb et al., 1999). We suspect that the Cherchen fault is a left-slip structure, based on its parallelism with the Altyn Tagh fault, its minimal vertical separation of Tertiary strata, and the left separations shown on the Xinjiang geologic map (Xinjiang Bureau of Geology and Mineral Resources, 1993).

Thrust Belts of Northern Tibet

Northwest-striking thrust and reverse faults in the Qilian Shan, Nan Shan, and Qiman Tagh (Fig. 1B) have been interpreted to be linked with the Altyn Tagh fault, causing an eastward decrease in slip rate along the strike-slip fault (Burchfiel et al., 1989; Chen et al., 2000; Meyer et al., 1998; Meyer et al., 1996; Tapponnier et al., 1990; Van der Woerd et al., 2001; Yin and Nie, 1996). The thrust front at the northeastern end of the Altyn Tagh system appears to have

migrated from southwest to northeast in discrete stages as the Nan Shan and Qilian Shan ranges were successively incorporated into the expanding Tibetan Plateau (Meyer et al., 1998; Tapponnier et al., 2001; Yin and Nie, 1996). The Akato Tagh bend lies to the northwest of the Qiman Tagh thrust belt (Fig. 1). Southwest-dipping thrusts along the northern margin of this thrust belt accommodate underthrusting of the Qaidam basin (Fig. 1) (Bally et al., 1986; Lee, 1984; Meyer et al., 1998; Song and Wang, 1993). Similarly, the Mahan-Tuoergan Shan (Fig. 1) overthrusts the northern margin of the Qaidam basin along a south-directed thrust system. Numerous active thrust and reverse faults accommodate additional shortening within the Nan Shan and Qilian Shan ranges (Meyer et al., 1998; Tapponnier et al., 1990).

NEOTECTONIC GEOLOGY OF THE AKATO TAGH

We have mapped active structures at four localities along the main trace of the Altyn Tagh fault (Fig. 2): Qingshui Quan (western segment), Pujilike (central segment), Liweiqiming Shan (eastern segment), and Kulesayi (eastern segment). At each locality, the geomorphology, Quaternary geology, and structures were mapped onto ~1:60,000-scale air photos. Field observations were then compiled on CORONA satellite images rectified to 1:100,000 topographic maps.

Quaternary Stratigraphy

Mapping and CORONA image analysis indicate that three main Quaternary units are widespread in the Akato Tagh area (Figs. 2 and 3). From oldest to youngest these units are Qo, Qm, and Qy. Qo deposits form deeply incised

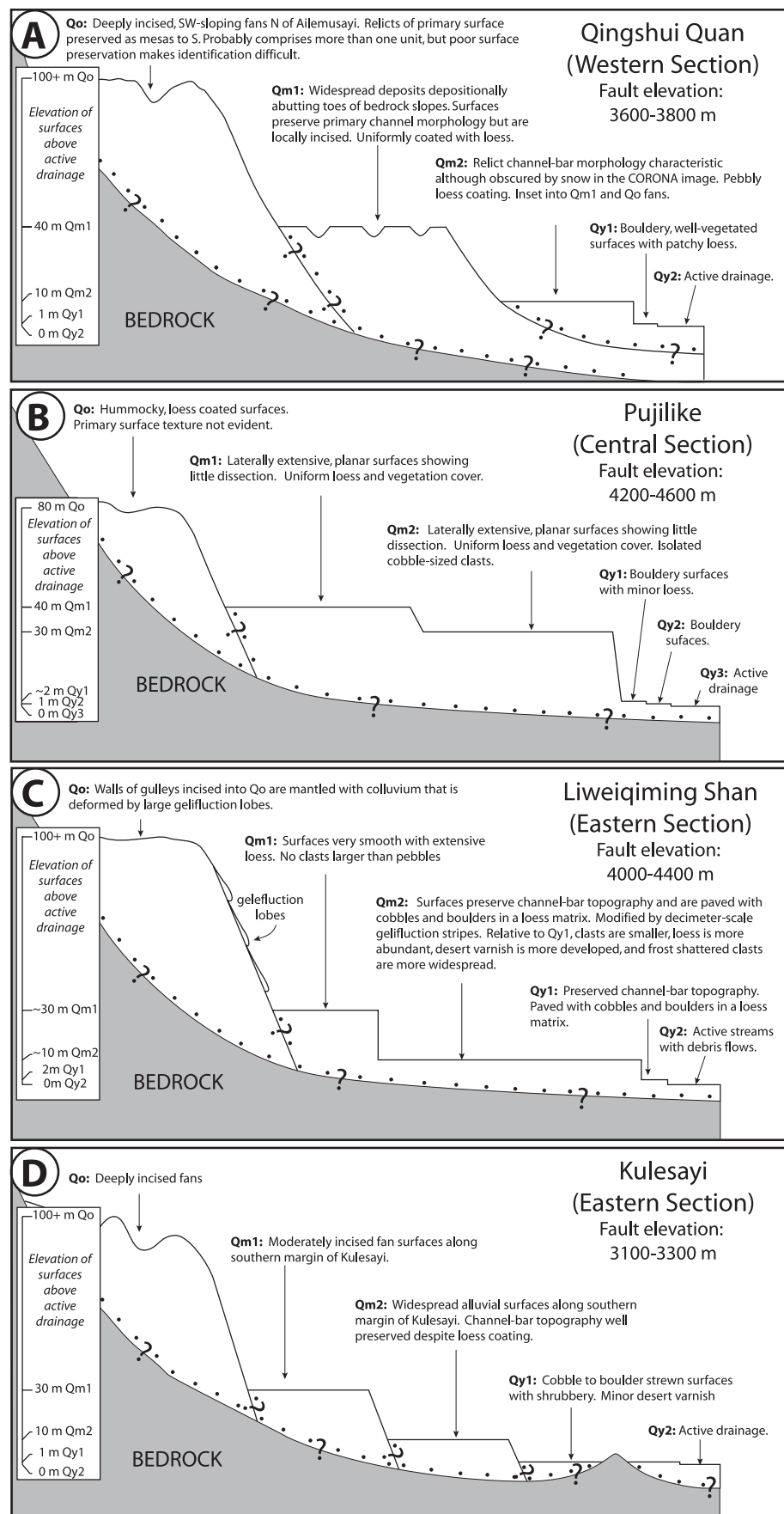


Figure 3. Schematic diagrams showing stratigraphy of Quaternary (nonglacial) surfaces and deposits in (A) Qingshui Quan, (B) Pujilike, (C) Liweiqiming Shan, and (D) Kulesayi study areas. Local Quaternary sequences were established using the heights of terrace surfaces, the degree of channel and bar preservation, thickness of loess covering, and the extent to which the terrace surfaces have been incised by younger drainage networks. Three main surfaces occur throughout the region, Qo, Qm, and Qy. In each map area we have broken these surfaces into subunits such as Qy₁, Qy₂, etc., where the numbers correspond to the sequence of development (i.e., Qy₂ is younger than Qy₁). Dots denote inferred depositional unconformities.

alluvial fans that stand ≤ 350 m above the active drainages and generally abut large glacier fields (Fig. 2), similar to ice-contact ‘morainic fans’ (Owen and Derbyshire, 1988). Qo fans overlap the range front to the north of Liweiqiming Shan and do not appear to be faulted on CORONA imagery (Fig. 2). Qm deposits are the most widespread unit in the Akato Tagh (Fig. 2), partially filling older valleys to form broad floors that depositionally abut the toes of adjacent hillsides, forming a sharp break in slope. Qm surfaces typically stand 10–40 m above the active drainages and preserve relict channel-bar topography, although some loess cover is present. Qy surfaces typically form narrow terraces that are inset into the Qm deposits. Bedrock is generally not exhumed within the floor of these Qy drainages, indicating that the Qm valley fill is at least 10–40 m thick.

Additional numerical subscripts (e.g., Qy₁, Qy₂, etc.) denote subunits, and follow the depositional sequence (i.e., Qy₂ is younger than Qy₁). This convention differs from neotectonic studies in which surfaces are numbered from lowest to highest elevation (e.g., Van der Woerd et al., 1998) and was adopted to highlight the sequence of surface formation. We do not correlate subunits (e.g., Qm₂) between the various study areas due to the probability that these units are not correlative.

We infer that all three main units are Quaternary due to the degree of surface preservation and gross similarity with dated units along the Altyn Tagh (Meriaux et al., 1997; Meriaux et al., 2000; Meriaux et al., 1998) and Kunlun faults (Van der Woerd et al., 2002). Relative ages between the surfaces can be established because the units are progressively inset and show different degrees of surface incision, loess cover, and preservation of original bar and swale topography.

Western Segment

Altyn Tagh Fault

We mapped the Qingshui Quan area (Figs. 2 and 4) to evaluate the significance of fault-perpendicular shortening along the principal trace of the Altyn Tagh fault outside the Akato Tagh bend. In this area, the active trace of the Altyn Tagh fault cuts all units except Qy₂ (Fig. 4A). The widespread Qm surfaces comprise two separate fans that are separated by a possible moraine that parallels the trace of the Altyn Tagh fault for ~5 km (Figs. 4A and 4B).

West of the inferred moraine, the trace of the Altyn Tagh fault strikes $\sim 066^\circ$ and lies at the base of a south-facing scarp that has been exposed by the east-directed displacement of the high-standing moraine to the south of the fault (Fig. 4A–4C). Shallow gullies incised

into the face of the scarp are consistently offset left-laterally 2–10 m (Fig. 4C). Where the trace cuts the moraine it bifurcates into at least three subparallel strands (Figs. 4A and 4B).

East of the moraine, the trace of the Altyn Tagh fault strikes $\sim 071^\circ$ (Figs. 4A and 4B) and is defined by a 1-km-long section of hummocks that lie parallel to the fault or trend slightly more eastward. These mounds deform Qm₂ and are 1–5 m high, ~30 m long, and up to 15 m wide. Folding of the Qm fan surfaces away from the trace is not obvious, nor are systematic vertical separations.

Structural Interpretation. In the Qingshui Quan area, the main trace appears to be characterized by pure strike-slip motion. This is best expressed by strike-slip motion along the 066° -striking fault segment in the western part of the area. In detail, however, the fault-parallel pressure ridges along the $\sim 071^\circ$ -striking eastern segment to the east indicate that there is a small component of fault-perpendicular shortening along this eastern reach. The magnitude of such fault-normal motion is presumably minor because these structures are small and the alluvial plains are not obviously folded.

Borderland Structures

Primary elements of a strike-slip system include the master fault and the flanking strike-slip borderlands (Jamison, 1991). For the present study, we define the borderlands as the 1–5-km-wide regions that flank the active master fault trace. Qo deposits are cut by linear scarps that strike $\sim 070^\circ$ and face northwest in the southeastern part of the area shown in Figure 4. As Figure 2 indicates, these scarps lie along strike from two active faults that are evident on both CORONA images and the published Active Fault map (Chinese State Bureau of Seismology, 1992). Traces of these faults trend parallel to the Altyn Tagh fault and deflect drainages sinistrally on the CORONA images. In the Qingshui Quan area, surfaces to the northwest of the scarps are lower than those to the southeast (Figs. 4A and 4B), suggesting that these faults have a south-side up, dip-slip component.

The thalweg of the Ailemusayi is deflected by several kilometers where it crosses the more northward of these two faults (Fig. 4A). If incision of the Ailemusayi drainage began prior to Qm₁ deposition, then this drainage has been offset left laterally 2.1 ± 0.3 km since the Qo surface was abandoned. While these deflections are compelling, they were not studied systematically in the field.

Structural Interpretation. The borderland faults are interpreted as dominantly left-slip faults with a small shortening component,

consistent with their more eastward strike relative to the 066° -striking fault segment that shows pure strike-slip motion.

Central Segment

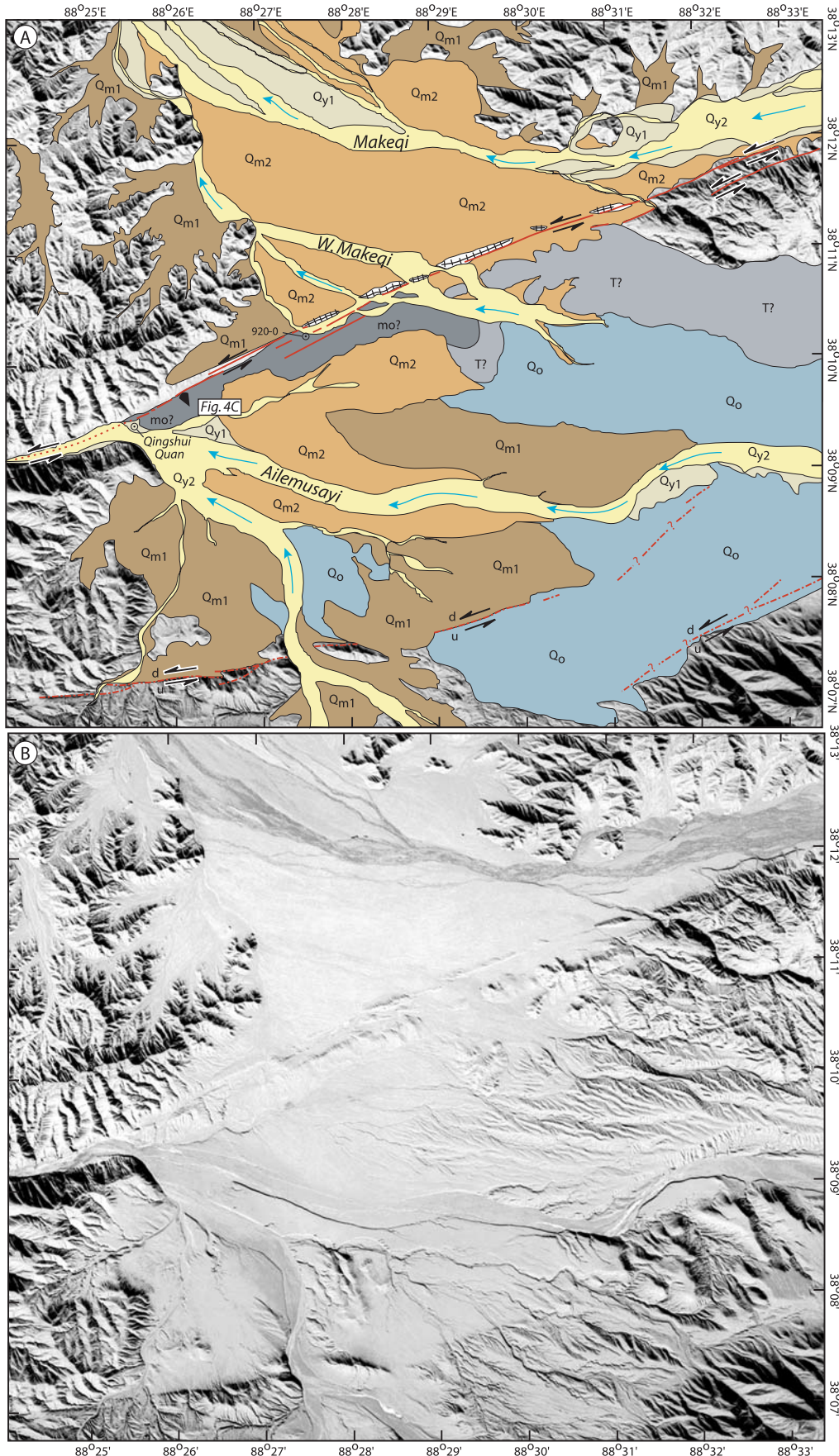
Pujilike Area

We mapped the Altyn Tagh fault where it crosses the head of Pujilike valley (Figs. 2 and 5A) to document active deformation along the main trace and look for evidence of fault-perpendicular shortening inside the bend. In the Pujilike area, the main trace strikes $\sim 090^\circ$ and cuts talus fields, Qo to Qm₂ surfaces, and at least two generations of moraines. Between stations ATF14 and ATF18 (Figs. 5A and 5C), the main trace is defined by a south-side up scarp with a meandering thrust trace at its base to the north, and a linear, left-slip trace at its head to the south (Fig. 5A). Despite along-strike variations in regional slope direction, this scarp consistently shows south-side up separation. At station ATF18 (Fig. 5C), a topographic profile across the scarp shows ~16 m of vertical separation. A maximum value for the horizontal component of separation since abandonment of the Qm₂ surface is 290 ± 50 m, as is indicated by the left-separation of the western edge of the Qm₂ surface near station ATF23 (Fig. 5A). A minimum value since abandonment of Qm₂ of ~46 m can be estimated from the deflection of the small gully that is incised into the scarp face at station ATF18 (Fig. 5C).

Structural Interpretation. If the fault at ATF18 dips 70° south, as is characteristic for fault zone fabrics in this area (see Cowgill et al., 2004), then ~4.6 m of fault-normal convergence is required to create the ~16 m of vertical separation seen at station ATF18 (Fig. 5C). Combining 4.6 m of convergence with the 290 ± 50 m of left-separation documented at station ATF23 (Fig. 5A) indicates the local slip vector trends $\sim 1^\circ$ oblique to the fault. Alternatively, combining fault-normal convergence with the 46 m deflection of the small gully suggests the slip vector trends $\sim 7^\circ$ oblique to the fault. In neither case is the slip vector as oblique as would be expected from the 20° bend angle for the Akato Tagh region.

Borderland Structures

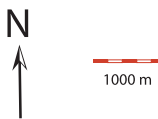
Keruke Fault Zone. The Keruke fault lies to the north of the active trace of the Altyn Tagh fault within the central segment of the Akato Tagh double bend (Figs. 2 and 6; see also Cowgill et al., 2004). Thalwegs of drainages incised into the Qo surface are deflected left-laterally by ~350 m where they cross the Keruke fault (northeast of station 828-3 in Cowgill et al., 2004), although Qm and Qy



EXPLANATION

SEE FIGURE 3 FOR UNIT DESCRIPTIONS
 (excluding T(?) bedrock)

Mapping by Eric Cowgill
 and Ramón Arrowsmith



Q _{y2}	Young, 2
Q _{y1}	Young, 1
Q _{m2}	Intermediate, 2
Q _{m1}	Intermediate, 1
mo?	moraine?
Q _o	Old
T?	Tertiary(?) redbeds

- Trace of Altyn Tagh fault, (well located, concealed)
- Interpreted fault (queried where uncertain)
d = down, *u* = up
- Pressure ridge
- Drainage direction
- field photo

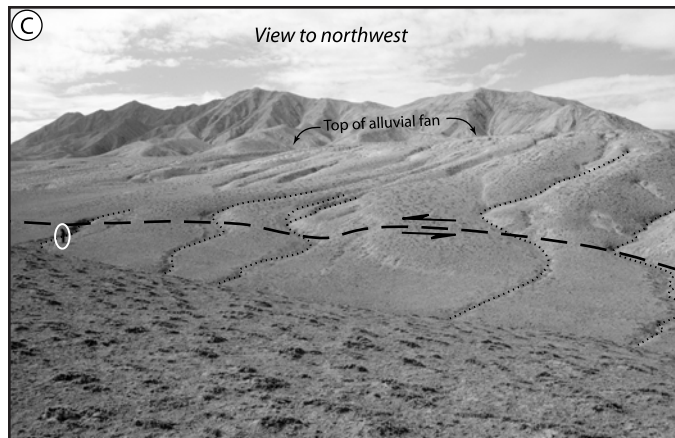


Figure 4 (on this and previous page). Active deformation and Tertiary(?) to Quaternary deposits along the Altyn Tagh fault in the Qingshui Quan area. (A) Neotectonic map and (B) uninterpreted CORONA photograph of the active trace of the western segment of the Altyn Tagh fault. Note the widespread distribution of Qm_2 -aged surfaces. (C) Photograph of the active trace of the Altyn Tagh fault showing systematic 3–10 m left-lateral drainage deflections. Person (circled) is ~1.8 m tall. Location of photograph is indicated in (A). Mapping in (A) was compiled on rectified CORONA photograph DS1105–1039DF146 taken November 6, 1968. Resolution of the CORONA image is ~8.5 m/pixel.

←

surfaces appear undeformed. Deflections of north-flowing streams systematically decrease toward the northeastern termination of the Keruke fault (Fig. 2). If these deflections formed due to slip along the Keruke fault, they suggest that offset decreases from southwest to northeast along strike, from 5000 m (red ticks on Fig. 2) to 3500 m (orange ticks) and finally to 2500 m (blue ticks).

Gasi and Anxi Faults. These faults lie to the south of the main trace of the Altyn Tagh fault, within the central segment of the Akato Tagh bend (Fig. 2). Brittle fabrics within these bedrock fault zones described in Cowgill et al. (2004) indicate they are predominantly left-slip faults. Although the Gasi fault does not cut Qm or Qy deposits, this fault coincides with a linear range front to the west of the Gasi Coal Mine and thus may still be active (Fig. 2 and Cowgill et al., 2004). On CORONA images this range front appears to connect with the southernmost active fault mapped in the Qingshui Quan area, as is shown in Figure 2. To the east of the Gasi Coal Mine, the Gasi fault lies within an east-west trending valley (Fig. 2 and Cowgill et al., 2004). This valley is morphologically similar to the young axial valley along the Altyn Tagh fault.

The Anxi fault also appears to be expressed geomorphically (Fig. 2). An east-west trending ridge of Jurassic rocks lies along the fault west of Gasi valley (Cowgill et al., 2004). This ridge has deflected both modern and Qm -aged

drainages, whereas a Qo surface is preserved to the south. Preservation of the Qo surface could indicate that the ridge is a pre- Qm shutter ridge or that the surface has been uplifted by post- Qo folding. The Qo surface is cut by a discontinuous, ~070°-striking, north-side up fault that crosses the Gasi valley and may merge with the Anxi fault farther east.

Two north-south trending elongate ridges stand above the Qm bajada south of the fault between the Xiong and Gasi valleys (Fig. 2 and Cowgill et al., 2004). Although the 1992 Chinese State Bureau of Seismology map (Chinese State Bureau of Seismology, 1992) shows both ridges as landslide deposits, we mapped these structures as moraines based on their morphologies, their excessive size relative to the proposed landslide source area, and the absence of clear headwall scarp. The moraines appear to have been offset left-laterally by ~8 km along the Anxi fault (Fig. 2).

Structural Interpretation. The Keruke, Gasi, and Anxi faults are interpreted as active left-slip faults inside the central segment of the Akato Tagh bend. No active thrusts were found within the borderlands along this segment.

Eastern Segment

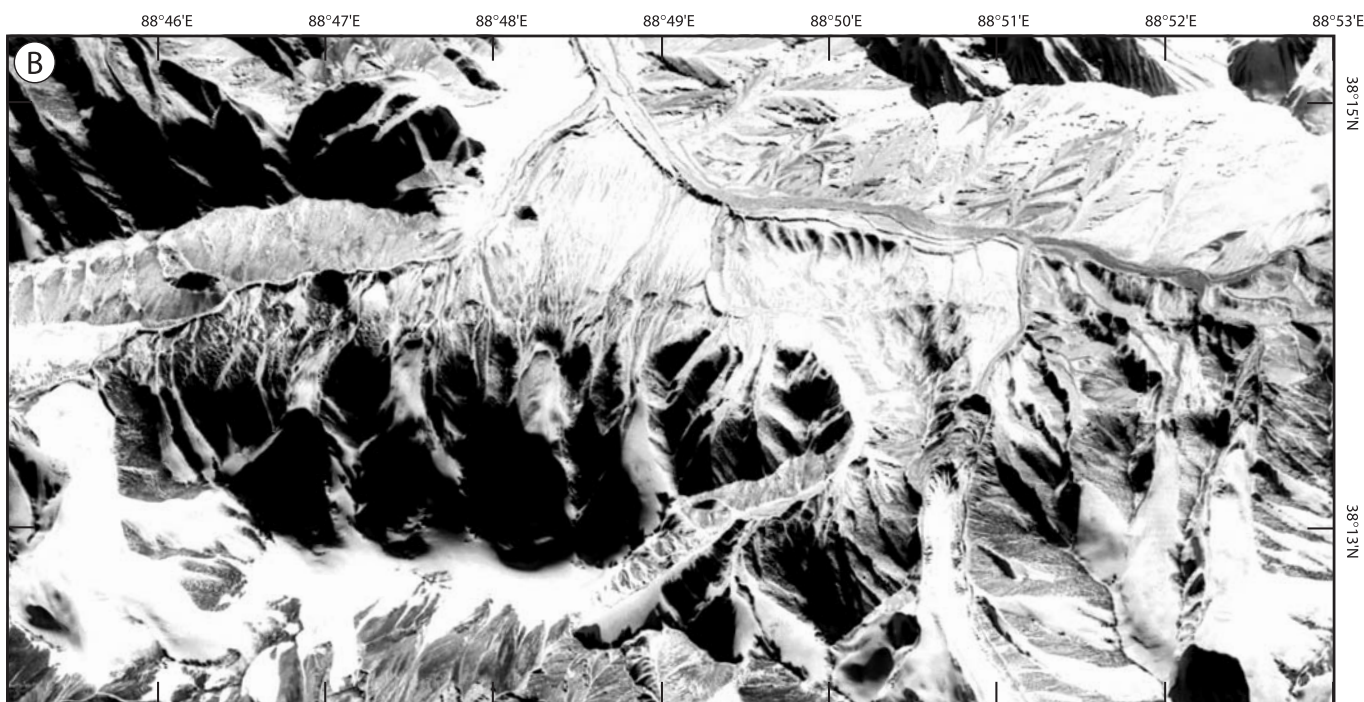
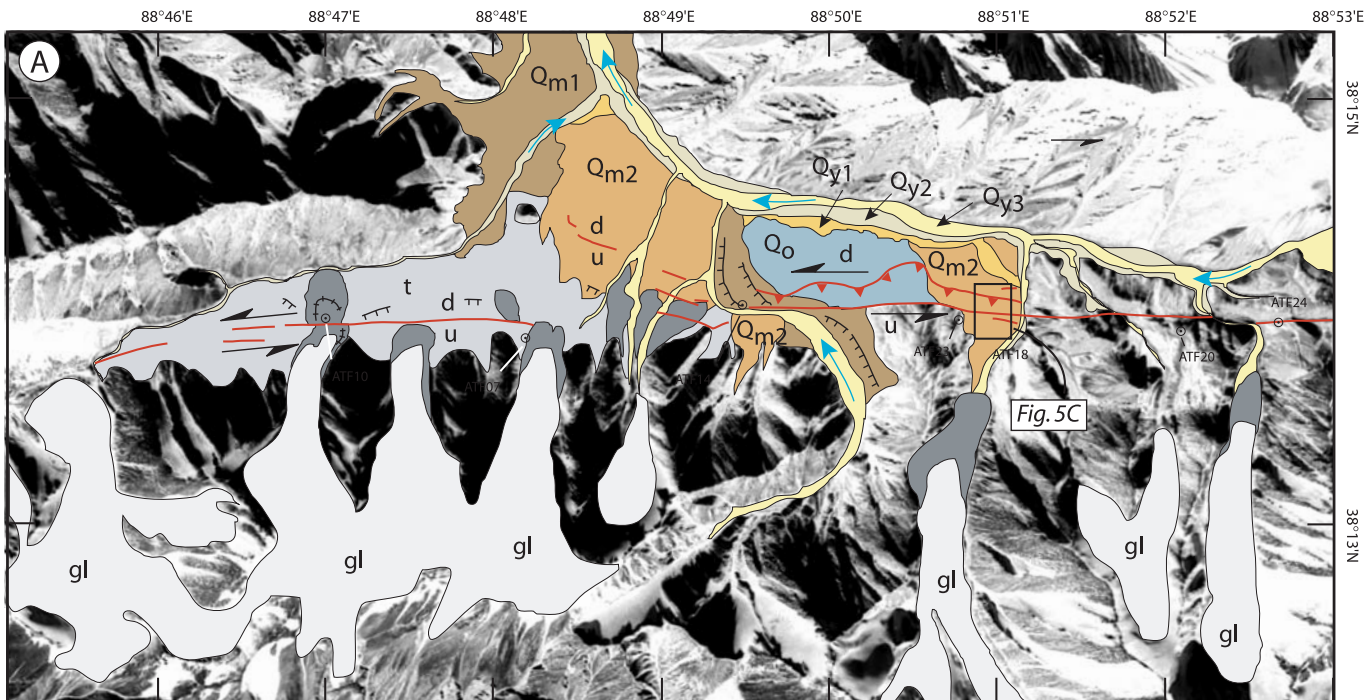
Liweiqiming Shan Area

We have mapped the Liweiqiming Shan area (Figs. 2 and 7A–7E) to investigate active deformation along the 065°–070° striking eastern

segment of the Altyn Tagh fault where it lies within the high topography of the Akato Tagh. In this area, there is a small but abrupt bend in the fault near site ATF39b (Fig. 7C). The fault trace strikes 066° and 072° to the west and east of this bend, respectively, with the eastern section showing consistent south-side up separation (Fig. 7B). Qy_1 and Qo surfaces south of the fault stand ~2 and ~30 m higher, respectively, than correlative horizons to the north (Fig. 7D), forming shutter ridges that shade the active trace on the CORONA image to the west of station ATF39 (Fig. 7B). In contrast, Figure 7E indicates that the fault trace to the west of this station is characterized by pure left slip: the trace cuts a broad, north-facing Qm_2 slope and is defined by numerous en echelon mounds, each of which is elliptical in plan view. The mound crests are cut by ridges and troughs that trend perpendicular to the long axes of the hillocks. Mounds on the Qm_2 surface are larger than those on the Qy_2 plain between stations ATF041 and ATF039, indicating the Qm_2 mounds have grown during more than one earthquake, assuming that these structures develop during coseismic slip.

Figure 7C indicates that deformation is complex at the junction between the 066° and 077°-striking fault segments. At the junction, the smooth, flat-lying surface of a Qm_1 terrace is cut by a set of northeast-striking tensional fractures. These furrows are 2–3 m deep, ~10 m wide, and are locally internally drained, indicating that they are not erosional. Material exposed in their walls is coarser grained, less varnished, and has much less matrix loess than the overlying Qm_1 surface. A 10-m wide, flat-lying bench of Qm_2 age stands ~7 m below the Qm_1 surface (Fig. 7C). In contrast to the loess-covered surface of Qm_2 , the Qm_1 bench is coated with pebbles and boulders and thus appears younger. For this reason, it is unlikely that the Qm_1 and Qm_2 surfaces are correlative and show south-side up displacement along the Altyn Tagh fault. The surface of the Qm_2 bench appears to roll over to the northwest, forming a monocline.

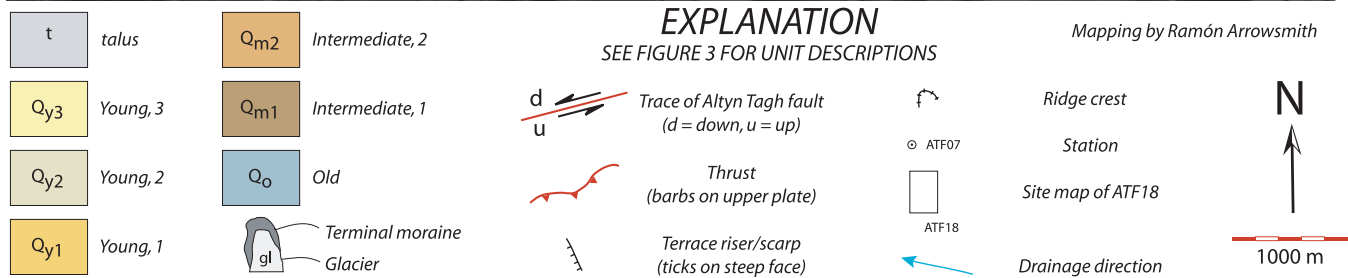
Structural Interpretation. Both the south-side up displacements (Figs. 7A and 7D) and the complex deformation at site ATF39b (Fig. 7C) probably result from oblique, left-reverse motion along the Altyn Tagh fault in the eastern part of the Liweiqiming Shan area. Local convergence across the fault at site ATF39b uplifted the shattered ridge relative to surfaces to the north. The monocline probably formed as a fault-bend fold, and we argue that the numerous extensional fractures that lie at a low angle to the active trace developed during gravitational collapse of the unsupported hanging wall scarp during and after the earthquake(s) that uplifted the Qm_1 surface. Broadly similar



EXPLANATION

SEE FIGURE 3 FOR UNIT DESCRIPTIONS

Mapping by Ramón Arrowsmith



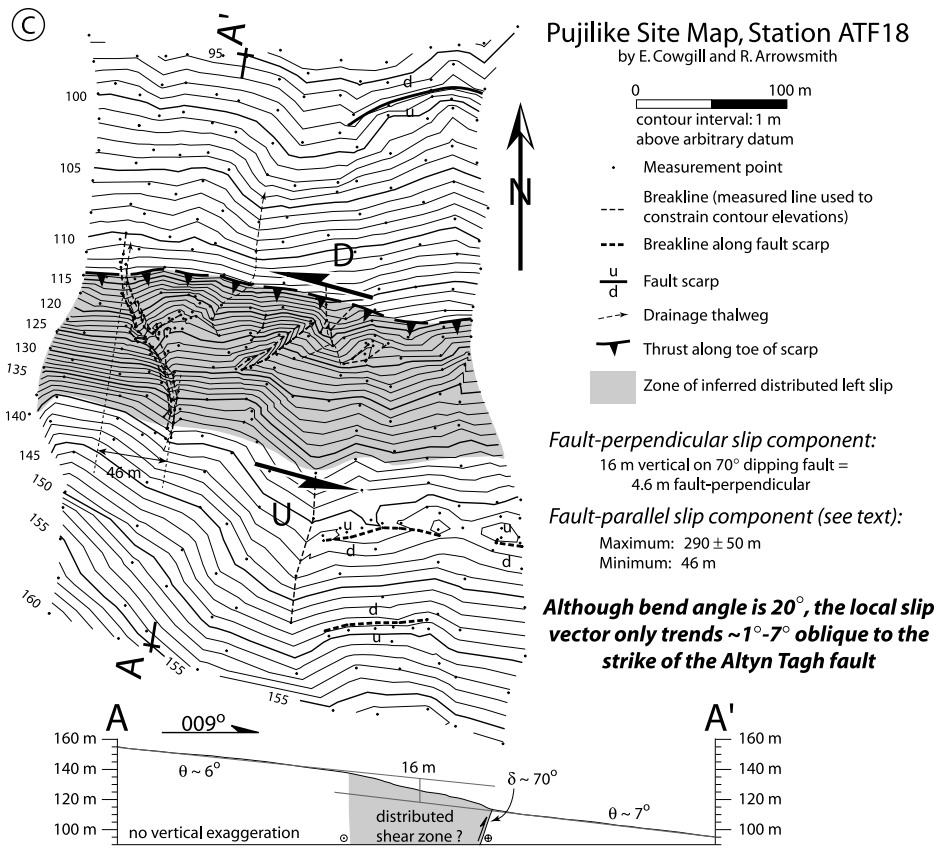


Figure 5 (on this and previous page). Maps of the active Altyn Tagh fault at the head of Pujilike valley, near the eastern end of the bend. (A) Neotectonic map and (B) uninterpreted CORONA image showing multi-stranded trace with straight strike-slip fault to the south and an arcuate thrust to the north. Base image is CORONA photograph DS1105–1039DF146 taken November 6, 1968. Image resolution is ~ 8.5 m/pixel. Geomorphic offsets are as follows. At station ATF10, both edges of a moraine are offset 70 ± 17 m, whereas at station ATF07 the western edge of a poorly preserved moraine is offset ~ 200 m. A glacially fed channel incised into older deposits between stations ATF20 and ATF24 appears to have been deflected left-laterally by 500 ± 40 m. At site ATF14, the thalweg of the deeply incised Qy₃ drainage shows a left-lateral deflection of 760 ± 130 m. Two terrace risers are present along the eastern edge of this drainage to the north of the fault, whereas a single riser is present to the south. If the single riser to the south of the fault matches with the eastern downstream riser, offset is ~ 800 m whereas a correlation with the western downstream riser would indicate ~ 1000 m of offset. All three risers curve as they approach the fault, becoming less oblique to the active trace. This curvature may indicate that the riser was partly offset prior to abandonment of the tread at the base of the riser. Both the deflection of the Qy₃ thalweg and the 800–1000 m riser offset have accumulated following the onset of incision of the Qm₁ surface. (C) Site map of the active fault trace at station ATF18 (see part A for location). Topographic profile constructed from the site map indicates ~ 16 m of south-side up vertical deformation. Scarp is incised by small gully that is deflected sinistrally by distributed wrenching. The gully is most deeply incised where it crosses the scarp, suggesting that incision and growth of the fault scarp were coincident. In addition, the central reach of the gully trends $\sim 45^\circ$ oblique to the topographic slope of the scarp face, in contrast to the upper and lower segments of the gully that trend perpendicular to the topographic gradient. We interpret this obliquity to result from left-shear of the thalweg. This site map and those in Figures 7C, 8C, and 8D were constructed using a Leica TCM 1100 total station and LISCAD software package with terrain modeling incorporating surveyed breakline constraints. Elevations are relative to an arbitrary datum.

structures formed by extensional collapse of the hanging wall during the 1988 Spitak earthquake (Philip et al., 1992).

Kulesayi Area

The Kulesayi area lies along the eastern straight segment of the Altyn Tagh fault, outside the high topography of the Akato Tagh (Figs. 2 and 8A–8B). In this area, the 065° -striking active trace of the Altyn Tagh fault is characterized by nearly pure left-slip, while 060° -striking fault systems in the adjacent borderlands show left-normal slip (Figs. 8 and 9). East of station 905-1, the fault cuts south-dipping Neogene strata in the crescent-shaped Kule ridge and then crosses a small playa within a pull-apart basin at station 912-0 (Fig. 8A). Gullies are deflected 16–40 m left-laterally around a series of shutter ridges that lie south of the 065° -striking trace at station 905-1 (Fig. 8C). The shutter-ridge crests lie at about the same elevation as the fault trace, suggesting pure left slip along the main fault at this locality (Fig. 8C).

At the playa site (station 912-0, Figs. 8A and 8D) the active trace bifurcates into two parallel, 060° -striking strands defined by en echelon sets of elliptical mounds (Fig. 8D). There is no obvious vertical component of motion along the Altyn Tagh fault at this site. Likewise, at station 906-4 (Fig. 8A) the Altyn Tagh fault cuts unconsolidated conglomerate, forming a zone of disrupted layering that is 1–2 m wide containing a ~ 10 cm thick zone of scaly, pebble-rich gouge striking 067° and dipping 78° south. Striae on faulted clasts within the zone indicate pure left slip.

Discontinuous $\sim 060^\circ$ -striking left-normal fault systems cut young alluvial fans north of the Altyn Tagh fault (Figs. 8A, 8E, and 9). Reconstruction of displaced gullies and ridges at station 906-2 (Figs. 8A and 9) indicates left-normal slip. Although gully exposures indicate 1–3 m of normal separation of the fan surface across these faults, the scarp faces are only 0.5–1.5 m high because the faults are partially buried by younger loess deposits (Figs. 9 and DR1).² Mismatches of detailed stratigraphy across these fault zones suggest a component of strike-slip motion.

The Kule ridge lies south of the active fault and comprises south-dipping, upper Neogene strata (Chinese State Bureau of Seismology, 1992; Liu, 1988; Xinjiang Bureau of Geology and Mineral Resources, 1993). The northern edge of this ridge is defined by an active, left-normal fault that strikes 062° and dips 66° north at station 903-3 (Fig. 8A). Striae at this site

²GSA Data Repository item 2004171, Figure DR1, is available on the Web at <http://www.geosociety.org/pubs/dr2004.htm>. Requests may also be sent to editing@geosociety.org.

indicate left-normal slip and plunge 62° toward 301° . Ridge lines terminate in triangular facets along the fault trace, and both drainages and the ridge lines show consistent left-normal separations with ridge crests showing $\sim 3:1$ ratios of dip-slip to strike-slip displacement.

Structural Interpretation. Active faulting in the Kulesayi area is expressed as pure left-slip motion along the main fault trace, which generally strikes 065° to 067° but is 060° at the playa site. In contrast, active faults both north and south of the fault generally strike more northward (060° – 062°) and show a normal component of motion.

INTERPRETED DEFORMATION PATTERN AND ITS IMPLICATIONS

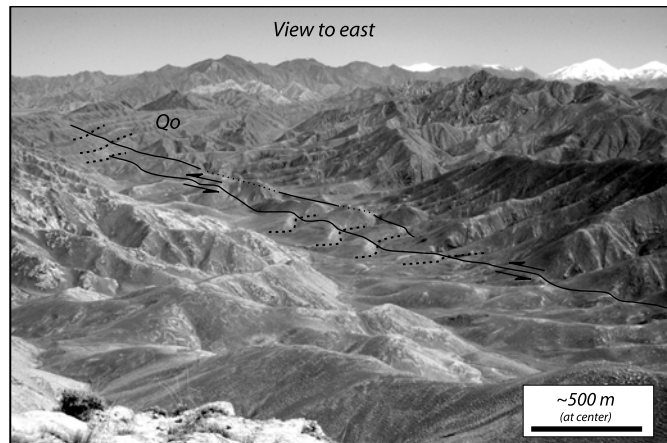
Two main conclusions can be drawn from our neotectonic mapping. First, patterns of active and bedrock deformation are broadly similar, although it remains unclear how active fault-perpendicular shortening is absorbed inside the bend. Second, the style of active faulting within the Akato Tagh bend is highly sensitive to fault strike, and we conclude that the western and eastern segments of the Akato Tagh bend are characterized by pure strike-slip motion. As our interpretations from the central segment indicate, these conclusions together imply that strike-perpendicular shortening across the Altyn Tagh system is probably minor.

Similarity of Deformation at Different Time Scales

Comparison of the active tectonics of the Akato Tagh with results from Cowgill et al. (2004) indicates that the patterns of active and bedrock deformation are generally similar. For example, the principal trace is dominantly a left-lateral strike-slip fault throughout the bend, even where it strikes east-west (see also the discussion of the neotectonic geology of the western segment). Second, both bedrock and active faults within the borderlands appear to be dominated by left-lateral, strike-slip motion, as opposed to thrusting (Fig. 2). Finally, both the active and bedrock deformation fields are partitioned along the east-west striking central segment of the Akato Tagh.

The Keruke and Kadzi faults provide the clearest examples of active strike-slip faulting within the borderlands (Fig. 2) but several of the bedrock faults described in Cowgill et al. (2004) also appear to be active (e.g., Gasi and Anxi faults). We suspect that young geomorphic offsets are not more abundant along the central segment because of the high local relief, the paucity of geomorphic surfaces within the bed-

Figure 6. Photograph of the Keruke fault (solid lines). Gullies incised into Qo deposits (dashed lines) show systematic left-deflections along a multi-stranded fault system. Relict Qo fan in the distance. See Figure 2 for location of photograph (station 815-3 in Cowgill et al., 2004).



rock drainages to record recent activity, and the brevity of the local geomorphic record.

The present investigation has failed to identify active structures that accommodate north-south, bend-perpendicular shortening, in contrast to Cowgill et al. (2004), which showed that such shortening has been absorbed by east-west trending folding. This problem is not surprising; inside a 20° bend such as the Akato Tagh, the rate of bend-perpendicular shortening is only $\sim 36\%$ of the rate of bend-parallel slip, presuming the western and eastern segments outside the bend show pure strike-slip motion. Thus while strike-slip faulting may be fast enough to outpace geomorphic resurfacing within the high-relief bend, bend-perpendicular shortening may be too slow to be expressed geomorphically. We suspect that active, bend-perpendicular shortening within the Akato Tagh is absorbed either by active folding, analogous to the pattern seen in Cowgill et al. (2004), or possibly by blind thrusts.

Although it remains to be determined how active bend-perpendicular shortening is absorbed within the Akato Tagh, the range does show evidence of active surface uplift (e.g., Fig. 2). Drainages are typically narrower and steeper inside the high topography of the bend than they are in the flanking regions. In addition, the Qm unit appears to have been tilted prior to incision and formation of the Qy tread in the Pujilike valley. Specifically, the Qy tread is inset into Qm deposits by ~ 30 m 1 – 2 km north of the principal fault (Fig. 5A) and the inset depth decreases downstream until the two surfaces eventually merge (Figs. 2 and 5; see also Fig. 4 in Cowgill et al., 2004).

Quaternary units are asymmetrically distributed around the bend, and thus surface and rock uplift rates may be highest within the two inside

corners in a pattern similar to that deduced in Cowgill et al. (2004). Valley-filling Qm deposits are absent from the narrow, steep-walled drainages in the southwestern and northeastern sectors of the Akato Tagh (Fig. 2), possibly indicating that these units were either stripped from the basins or never deposited because surface uplift rates are high in these areas. In contrast to the Qm deposits, the Qo fan complexes are most prevalent adjacent to the two inside corners. If the formation of these deposits is genetically related to the adjacent glaciers (e.g., Owen and Derbyshire, 1988) then their greater concentration adjacent to the inside corners may indicate rapid rates of rock uplift and glacial erosion in these areas.

Clearly some of this geomorphic variability is probably due to heterogeneous bedrock lithology, along-strike variations in precipitation, or non-uniform drainage response to changes in sediment supply, stream power, or local base level. However, we suspect that active deformation has exerted a first-order control on the drainage network within the Akato Tagh bend. Bedrock lithologies are grossly uniform along strike (Cowgill et al., 2004), and the bend is small enough that along-strike variability in precipitation is probably minor. Finally, the stratigraphy and morphology of Quaternary deposits is generally similar in the four mapped areas (Fig. 3), suggesting these regions have experienced grossly similar sequences of Quaternary deposition and incision.

The Optimal Strike-Slip Orientation (065° – 070°)

If the style of faulting along the main fault trace can be integrated with the pattern of deformation in the flanking borderlands, then it

should be possible to capture the total displacement field of north Tibet and Qaidam relative to the Altyn Tagh range. Our mapping indicates that pure strike-slip motion along the main trace only occurs along a narrow range of fault orientations (065° – 070°). We interpret regional active deformation around this bend to reflect pure strike-slip motion along the $\sim 065^{\circ}$ – 070° -striking western and eastern fault segments, accompanied by partitioned transpressional deformation along the $\sim 087^{\circ}$ -striking central segment. Thus, north Tibet and Qaidam move toward 065° – 070° relative to the Altyn Tagh range.

Figure 10 shows a compilation of our field observations from the Akato Tagh and illustrates that structural style is highly sensitive to fault orientation. Pure left-slip characterizes sections of the Altyn Tagh fault that strike 065° – 067° (i.e., Kulesayi, the western parts of the Qingshui Quan, and Liweiqiming Shan map areas). Deviation from this optimal orientation by just a few degrees introduces an oblique component of slip. Transpression characterizes sections that strike 071° to 072° (i.e., in the eastern parts of the Qingshui Quan and Liweiqiming Shan map areas, Figs. 4A and 7A) while transtension occurs along borderland faults that strike more northward (060°) in the Kulesayi area (Fig. 8A). The playa site (Figs. 8D and 10) is the only locality that does not fit this pattern. The slip directions along the active faults show a sensitivity to fault orientation that is not evident along the bedrock structures as described in Cowgill et al. (2004). This sensitivity is probably due to the shorter record and thus lower finite strain recorded by the Quaternary deposits relative to the more complex finite record of deformation preserved within the bedrock fault zones.

Although we have looked for evidence of slip partitioning and active shortening within the borderlands adjacent to the $\sim 065^{\circ}$ – 070° -striking western and eastern segments of the Akato Tagh, we have found no such deformation. For example, we have found no evidence of active folding in the borderlands of the Qingshui Quan, Liweiqiming Shan, and Kulesayi map areas. Although borderland faults have a dip-slip component in the Qingshui Quan and Liweiqiming Shan areas, this observation is consistent with the oblique strike of these faults relative to the 065° – 070° optimal orientation for pure strike-slip faulting shown in Figure 10. As a result, we do not think these faults indicate the western and eastern segments of the bend are transpressional.

Implication: Minor Transpression along the Altyn Tagh System

Although it is commonly held that the Altyn Tagh system is transpressional (e.g., Meyer et

al., 1998; Tapponnier et al., 2001; Wittlinger et al., 1998) the present study and previous work together fail to support this idea. Thus, we speculate that the Altyn Tagh system is characterized by essentially pure strike-slip motion between Tibet and Tarim, as recent geodetic results have shown (Bendick et al., 2000; Shen et al., 2001).

Clearly there should be structural evidence for northwest-southeast shortening across the Altyn Tagh system if it is transpressional. Results from the present study imply that such shortening does not occur along the principal active trace. Topographically, the Akato Tagh is similar to the three other double restraining bends shown in Figure 1: elevated areas are concentrated along the central segments of the double bends while topography is minor along the flanking fault segments outside the bend. These adjacent segments generally strike close to the 065° – 070° optimal orientation for pure strike-slip motion determined within the Akato Tagh bend. As such, it is likely that they too are characterized by essentially pure left-slip.

The apparent lack of northwest-southeast shortening along the main active trace implies that this shortening must be absorbed elsewhere within the Altyn Tagh system if it is indeed transpressional. For example, although the central San Andreas fault in California is characterized by pure right-slip, young folds occur adjacent to the fault in the Coalinga area and attest to net transpression (e.g., Jamison, 1991; Miller, 1998; Teyssier and Tikoff, 1998). A number of studies have interpreted the North Altyn fault (Fig. 1) as a thrust that accommodates shortening across the Altyn Tagh system (e.g., Avouac and Tapponnier, 1993; Burchfiel et al., 1989; Peltzer and Saucier, 1996; Wittlinger et al., 1998). However, no field measurements have been reported to support this idea, and recent work along a 120 km long reach of the fault has clearly demonstrated that strike-slip motion predominated over thrusting (Cowgill et al., 2000). In particular, measured slip directions trend 045° to 060° along a fault that strikes 060° and dips $\sim 65^{\circ}$ south.

Although more data are needed from the Altyn Tagh system before the importance of regional transpression can be fully evaluated, the simplest analysis of the existing observations suggests that the system is dominated by strike-slip motion rather than transpression. This speculation is supported by recent GPS results indicating only minor northwest-southeast shortening. Shen et al. (2001) demonstrated that Tarim and Qaidam show undetectable internal deformation while the intervening 070° -striking Altyn Tagh fault system accommodates 9 ± 2 mm/y of left slip and 0 ± 2 mm/y of northwest-southeast

shortening. Likewise, by resolving slip rates reported by Bendick et al. (2000) onto the 070° -striking Altyn Tagh system, we find that there should be 9.5 ± 5.1 mm/y of left slip and only 1.4 ± 1.2 mm/y of northwest-southeast convergence, consistent with the rates reported by Shen et al. (2001). Thus, both our investigations and the GPS studies give a similar picture of essentially pure strike-slip motion along 065° – 070° striking sections of the Altyn Tagh system, suggesting that the “instantaneous” kinematics of the Altyn Tagh fault determined by the GPS surveys may be representative of the late Tertiary-Quaternary motion.

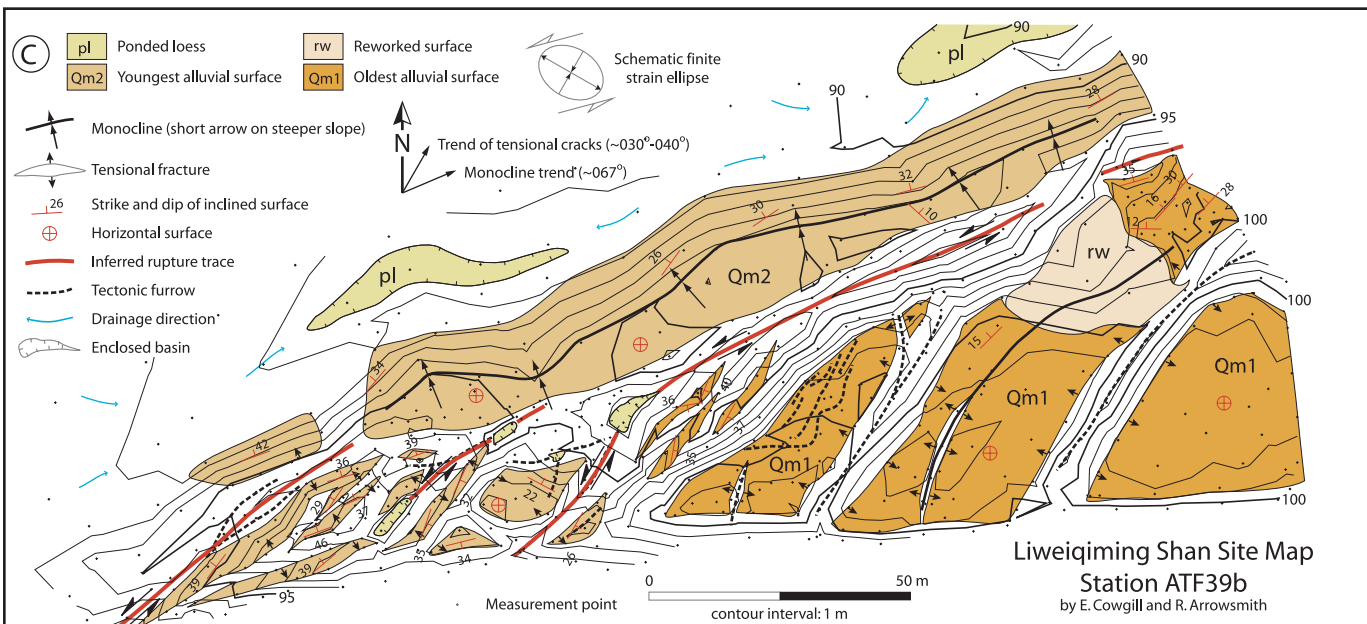
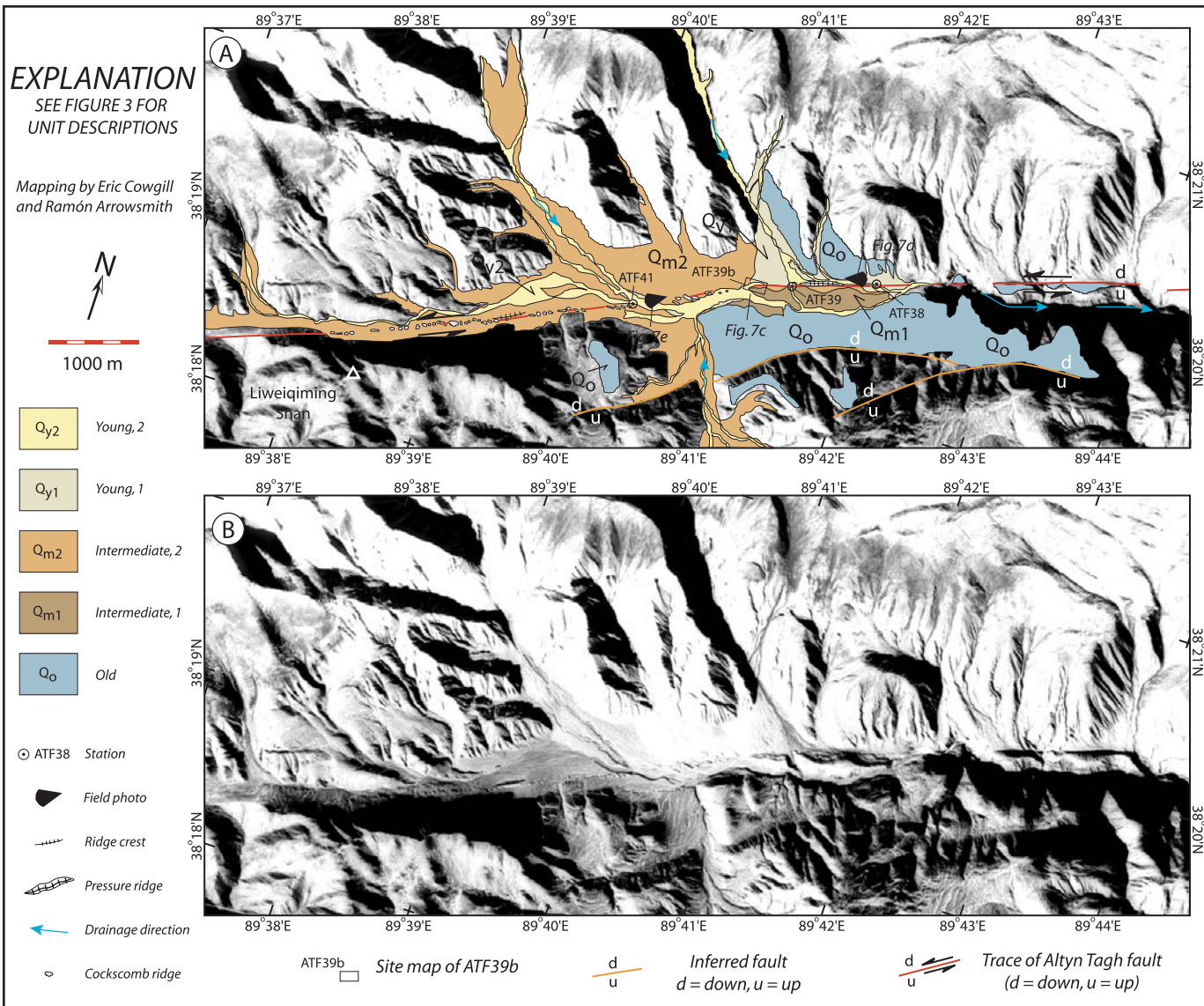
DISCUSSION: STRAIN-HARDENING

The lateral extrusion hypothesis requires that the continental lithosphere undergoes strain-softening to produce long-lived, fast-moving faults that accumulate large magnitudes of displacement. But, if faults are weaker than the blocks they bound, what causes new strands to break, thereby producing a broad zone of subparallel strike-slip faults such as the Altyn Tagh system (Fig. 1)? In this section we argue that the Altyn Tagh system appears to have developed by the sequential formation and abandonment of short-lived fault strands, and therefore reflects net strain hardening, rather than the softening required by the extrusion hypothesis. In detail we suggest that both softening and hardening processes are likely to have been active simultaneously during the evolution of this fault system, in which case the net behavior of the system reflects the outcome of a competition between softening mechanisms, such as reduction in bend angle by vertical-axis rotation (e.g., Cowgill et al., 2004), and hardening processes, such as growth of restraining-bend topography or material hardening of fault gouge. Net strain hardening of the system produces deformation that is spatially localized over the 1–5 m.y. during which an individual fault is active but distributed at the 10–100 m.y. time scale that corresponds to the duration of a continental collision.

Why are Fault Systems Complex?

Major strike-slip systems often comprise geometrically complex networks of subparallel fault strands. In addition to the Altyn Tagh fault (Fig. 1), the central San Andreas fault in California and the northeastern Alpine fault in New Zealand are also geometrically complex. As Figure 11 illustrates, three end-member scenarios can explain how such systems form: strain hardening, strain softening, and stable yielding.

In the case of net strain-hardening (Fig. 11A), a broad fault system develops by the sequential



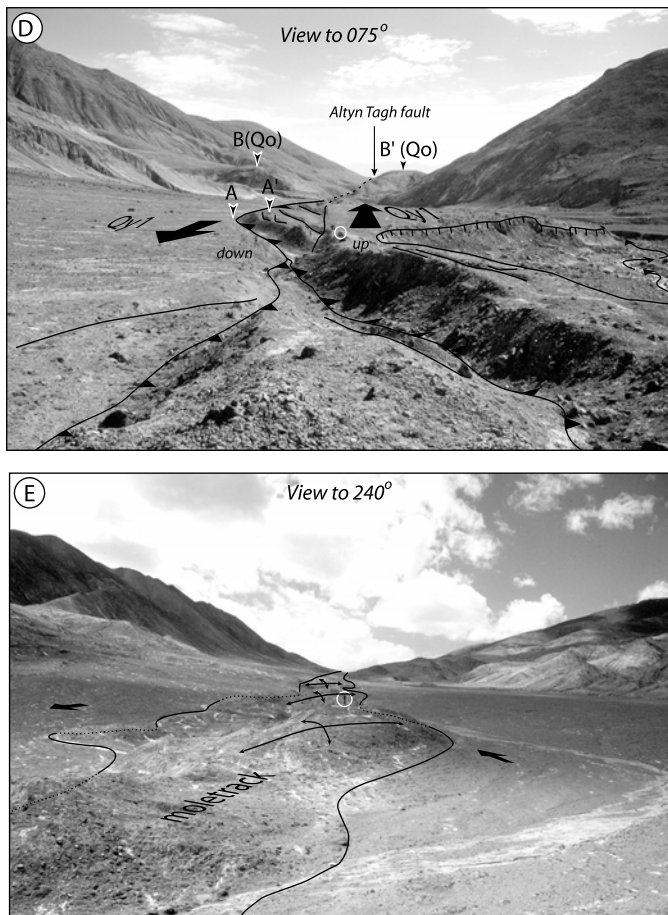


Figure 7 (on this and previous page). Expression of active deformation along the Altyn Tagh fault in the Liweiqiming Shan area. (A) Neotectonic map and (B) uninterpreted CORONA image. To the east of station ATF39b the fault strikes 072° and shows a consistent south-side up component of deformation. West of station ATF39b the fault trace strikes 066° and is defined by en echelon cockscomb ridges. Map base is rectified CORONA scene DS1102–1039DA073, taken December 12, 1967. Image resolution is ~ 8.5 m/pixel. (C) Detailed map of site ATF39b showing north-facing homoclinal and en echelon brittle fractures related to left-reverse motion on the Altyn Tagh fault. Schematic strain ellipse is derived from the orientations of the master strike-slip fault and the en echelon tensional fractures cutting the Qm_1 and Qm_2 surfaces. Note that the ellipse is schematic and should not be interpreted as a finite strain measurement. See text for explanation. (D) Photograph of the active trace east of station ATF39b showing south-side up separations of surfaces between points A–A' and B–B'. Circled box is 0.5 m tall. (E) Photograph of the mole track to the west of station ATF39b showing en echelon cockscomb ridges (solid lines with arrows). Circled person for scale.

←

formation, dominance, and then death of individual fault strands. Each strand is short-lived relative to the shear zone, and only one fault strand is dominant at any given time. Thus, the active trace is younger than the system as a whole and both the total number of strands and the overall width of the shear zone increase with time. This first scenario predicts that continental deformation is localized at short time scales but distributed at longer intervals. In the case of strain-softening (Fig. 11B), deformation

initiates within a diffuse zone but is rapidly focused during progressive deformation onto one principal fault. In this case, long-term continental deformation is localized along narrow fault zones. In the case of stable yielding (Fig. 11C), deformation starts on a single fault but new faults develop adjacent to this strand as deformation progresses, so that both the number of active fault strands and the width of the shear zone increase as slip accumulates. At any given time, all of the faults within this shear zone are

active and the main trace is active for the duration of deformation. This third mode of deformation is produced in analytical and numerical models in which a discrete mantle fault is overlain by a linearly viscoelastic crust with depth-dependent viscosity (Roy and Royden, 2000a, 2000b). In these models, broad upper crustal shear zones are produced by diffusion of slip within the weak lower crust, and the location of the crustal shear zones is therefore fundamentally controlled by the location of the underlying mantle fault that drives the deformation.

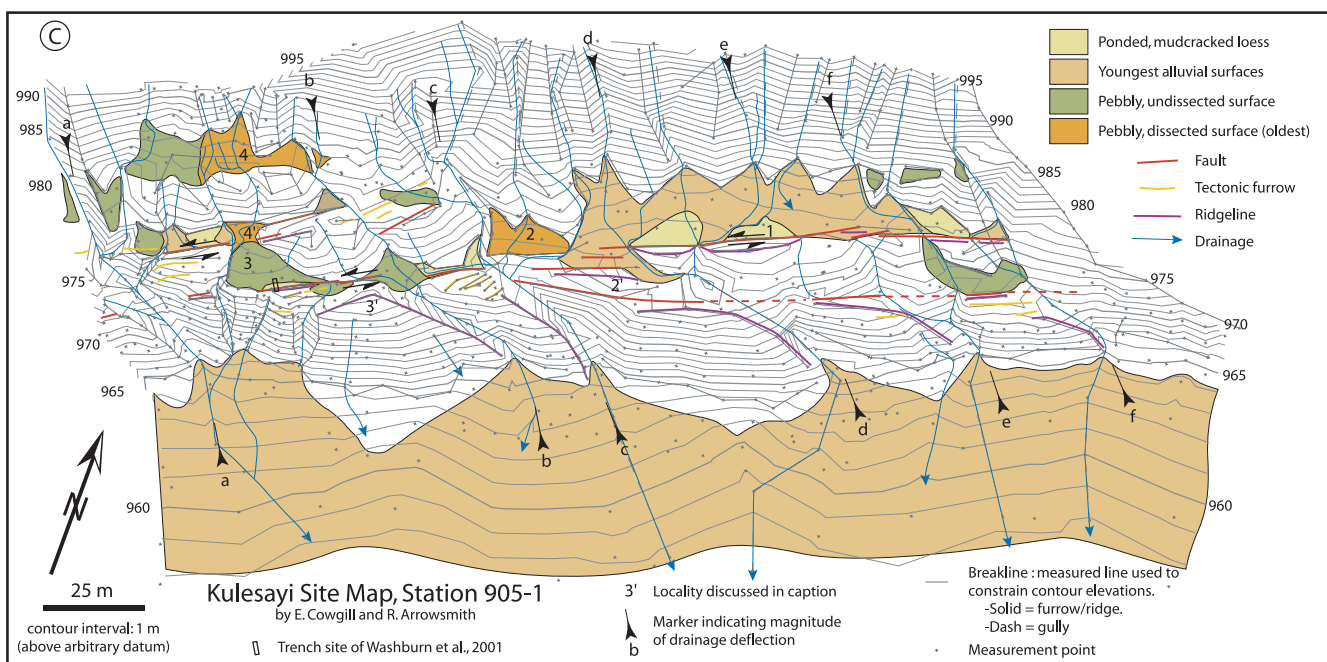
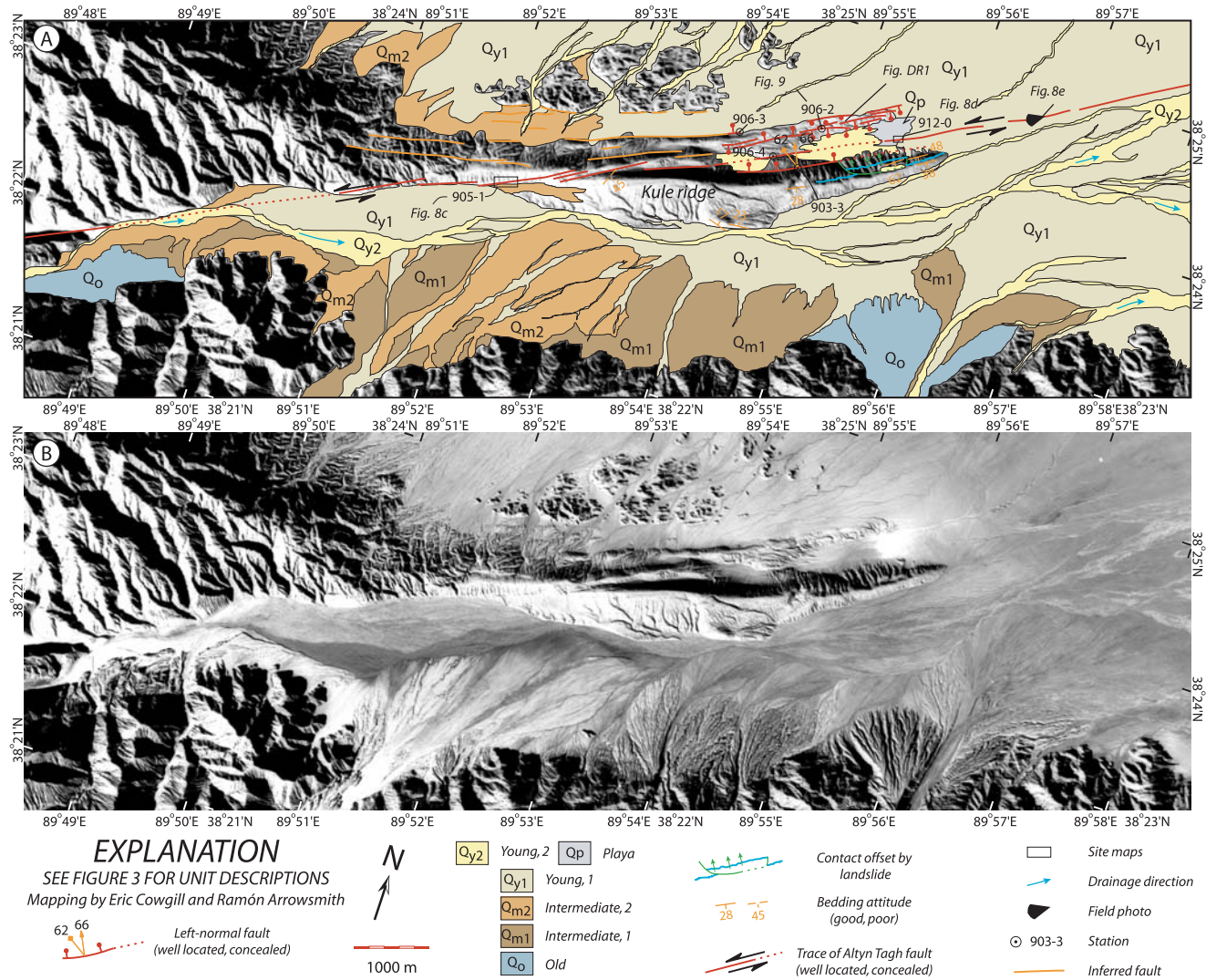
Figure 11 demonstrates that it is possible to distinguish between these three scenarios based on the age of the main trace relative to the system as a whole: in the first case the main trace is much younger than the system that contains it, whereas in the other two the system and the main trace have the same age. Cowgill et al. (2004) presents four estimates for the age of the Akato Tagh bend and shows that the bend is probably only a few million years old, significantly younger than the ca. 49 Ma system that contains it. But does the youthfulness of the bend indicate that the active trace is also young or could the bend reflect recent deformation of a long-lived fault trace? Addressing this question requires understanding how the bend formed.

How do Double Bends Form?

Here we argue that formation of a young bend by recent deformation of an old fault is inconsistent with the pattern of deformation described above in the neotectonic geology section. Therefore, we speculate that both the main trace and the four right-stepping bends formed by coalescence of R- and P-shears (Fig. 12), in which case the main fault is only a few million years old.

As Figure 12 indicates, we see three main ways to make the right-stepping double bends along the Altyn Tagh fault. One possibility is that the bends first formed as a discontinuous set of en echelon R-shears that eventually linked via bridging P-shears (Fig. 12A) in a sequence that is commonly observed in analog models (e.g., Friedman et al., 1976; Tchalenko, 1970). Cunningham et al. (1996) proposed a similar explanation for the North Gobi-Altai fault system, which they argued developed by the growth and coalescence of a series of transpressional bends within an initially discontinuous set of en echelon strike-slip faults in southern Mongolia (Cunningham et al., 1996).

A second option is that the four double bends result from recent deformation of the active trace by block motions. Each bend is located along the north end of a northwest-southeast striking thrust belt (Fig. 1). As Figure 12B indicates, if



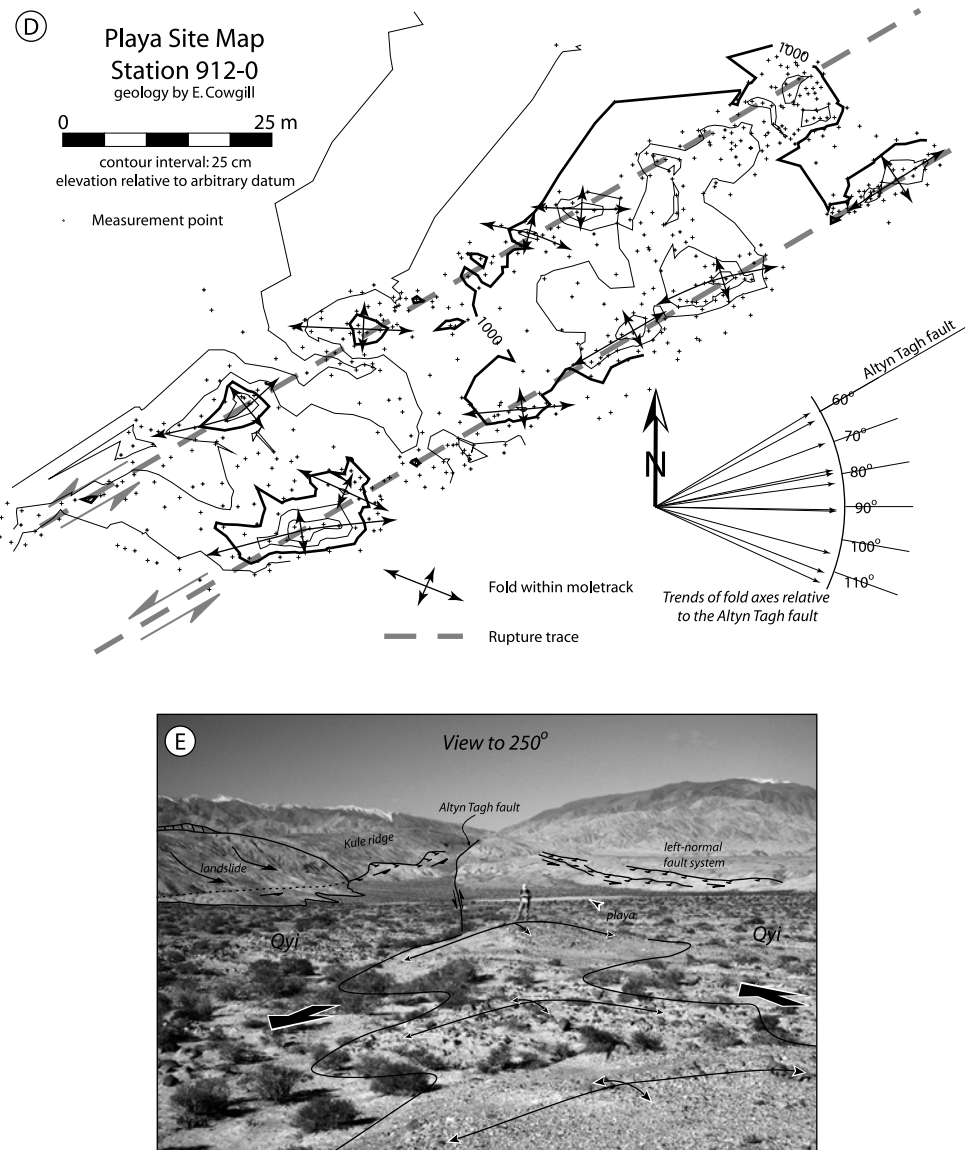


Figure 8 (on this and previous page). Active deformation in the Kulesayi area to the east of the Akato Tagh. (A) Neotectonic map showing 065°-striking main trace flanked to the north by 060°-striking left-normal faults. Kule ridge to the south of the main fault has a steep northern face defined by a left-normal fault. Neogene(?) sediments within this ridge may have been deposited at the toe of the mountain in the northwest corner of the image. Exposures along the north face of Kule ridge reveal a lower unit of predominantly red siltstone and pebbly sandstone that is capped by a boulder lag horizon and overlain by an upper interval of pebble to cobble conglomerates. East of station 903-3, the normal fault at the base of Kule ridge is buried by a landslide slump block that has also offset the sand-conglomerate contact within the Neogene strata (Fig. 8A). Base image is a portion of rectified CORONA scene DS1102–1039DA073, taken December 12, 1967. Image resolution is ~8.5 m/pixel. (B) Uninterpreted CORONA image. (C) Site map of the Altyn Tagh fault at station 905-1, west of Kule ridge. Lettered arrows indicate drainages that have been offset and/or deflected left-laterally up to ~90 m. Northeast-directed motion of shutter ridges south of the fault has produced several generations of ponded and incised deposits north of the fault. Mud-cracked loess and fans at locality 1 are actively aggrading behind ridge 1'. Pebby but undissected surfaces at site 2 probably accumulated behind ridge 2', while older, more heavily dissected surfaces at site 3 probably accumulated behind ridge 3'. Correlation of surfaces at 4 with those at 4' may reflect either shallow slumping or that the fault has a north side up (extensional?) component of slip. (D) Site map of the Altyn Tagh fault where it crosses the playa north of Kule ridge. Trace is defined by en echelon sets of mounds that are typically ~40–60 cm high, ~15 m long, and ~5 m wide, with long axes that trend up to 50° more eastward than the fault. Thinly laminated lacustrine sediments are complexly folded within the mounds. As Molnar et al. (1987a, 1987b) noted in their description of this area, the orientation of these structures relative to the fault indicates left-slip. Topographic base map prepared by Elizabeth Catlos and Zhang Shuanhong. (E) Photograph of the basin to the north of Kule ridge, looking to the west along the Altyn Tagh fault; person for scale. En echelon mole tracks (outlined in solid lines with double-headed arrows showing fold axes) in foreground. Left-normal fault on the north side of Kule ridge is buried by younger landslide slump. Black ticks indicate headwall scarp.

the blocks that lie to the south of the Altyn Tagh fault move obliquely relative to the fault, they could have produced a series of right-stepping bends where the corner of each block converged upon the Altyn Tagh range. The relative block motions required to deform the fault trace in this way produce left-reverse motion along both the northwest-striking thrust belts and the Altyn Tagh fault. The velocity diagram in the initial configuration in Figure 12B demonstrates that dextral bending of the Altyn Tagh fault does not require dextral motion along the north Tibetan ranges (see also caption to Fig. 12). However, this block model has two major problems. First, it is unclear if the thrust belts are linked with the Altyn Tagh fault because in general they are separated from one another by a large valley that parallels the Altyn Tagh fault (Fig. 1; see also, Robinson et al., 2003). Second, the model requires that the 065°-striking sections of the Altyn Tagh fault are transpressional. However, the western and eastern fault segments have no clear component of fault-perpendicular shortening (see the neotectonic geology section above). Likewise, the Xorkol segment is similarly oriented but is clearly transtensional (Washburn et al., 2003).

A third possibility is that the right steps developed during eastward propagation of the Altyn Tagh fault (Fig. 12C). Bayasgalan et al. (1999) suggested that thrust-terminated strike-slip faults may propagate in discrete jumps because elongation of the strike-slip fault is not required until the thrust front steps basinward. Although this mechanism explains the linkages between the thrusts and the strike-slip fault, it does not explain why those linkages are systematically right-stepping. Meyer et al. (1998) have proposed that the thrusts systematically curve into the Altyn Tagh fault due to their initiation within an anomalous stress field at the tip of the Altyn Tagh fault during its eastward propagation. It may be that interaction between the anomalous stress fields at the two fault tips causes the propagating strike-slip fault tip to step right, toward the thrust tip (Fig. 12C). However, this third model requires that the bends date from the time of initial propagation of the Altyn Tagh fault, around 49 Ma (e.g., Yin et al., 2002 and references therein), which is much earlier than the few million year age estimates for the Akato Tagh bend reported in Cowgill et al. (2004).

Only the first scenario (Fig. 12A) can explain both the pattern of deformation within the Akato Tagh bend and the discrepancy in ages between the bend and the fault system as a whole. But, in order for this first scenario to work, the active trace of the Altyn Tagh fault can be no older than the Akato Tagh bend. For this reason, we suggest that young age of the Akato Tagh bend

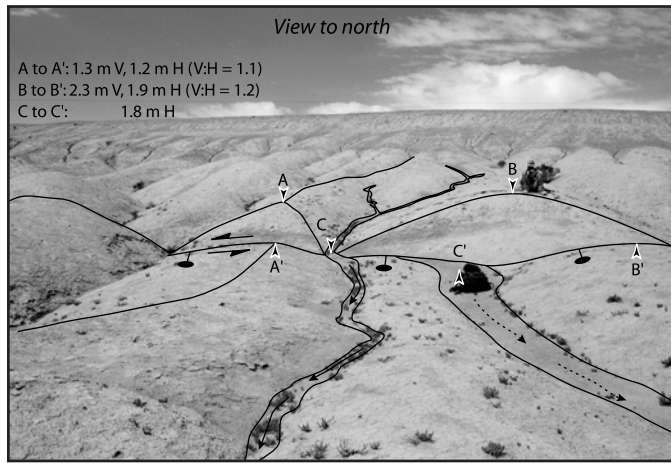


Figure 9. Photograph of the left-normal fault system in the northern part of the Kulesayi area; person for scale. Left-normal fault scarp cuts loess-rich deposits at station 906-2 (see Fig. 8A for location). This site appears to record two earthquakes. Measurements made with a tape and compass at this locality indicate that the western ridge (A–A') preserves 1.3 m of vertical and 1.2 m of left slip, the eastern ridge (B–B') shows 2.3 m of vertical and 1.9 m of left slip, and the offset thalweg shows 1.8 m of horizontal offset. Note the left deflection of the thalweg at the head of the offset drainage. Although the western ridge is offset less than either the eastern ridge or the thalweg, the ridges show similar ratios of vertical to horizontal offset. Our interpretation is that this site records offsets from two earthquakes. Both ridges (A–A' and B–B') and the thalweg record the most recent earthquake, which appears to have had vertical and left-lateral offsets of 1.3 m and 1.2 m, respectively. The penultimate earthquake had vertical and left-slip offsets of 1 m and 0.7 m, respectively, as recorded by the eastern ridge and the beheaded gully. The left-deflection of this gully was probably produced by this earlier event. Evidence of recent rupture within the left-normal set of faults extends at least as far north as station 906-3 (Fig. 8A), where there is a sharply defined scarp ~50–60 cm high.

NORTH

- Transtensional
- Pure left-slip
- - -→ Transpressional

Pure Left-Slip: ~065°

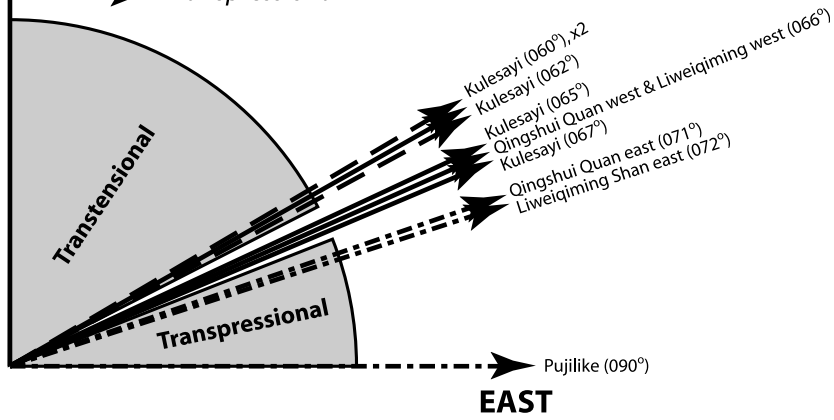


Figure 10. Diagram showing how structural style varies as a function of fault orientation. Only fault segments that strike N65°E ± 5° show pure left-slip kinematics. Faults that strike more eastward have a transpressional component whereas faults that strike more northward are generally transtensional.

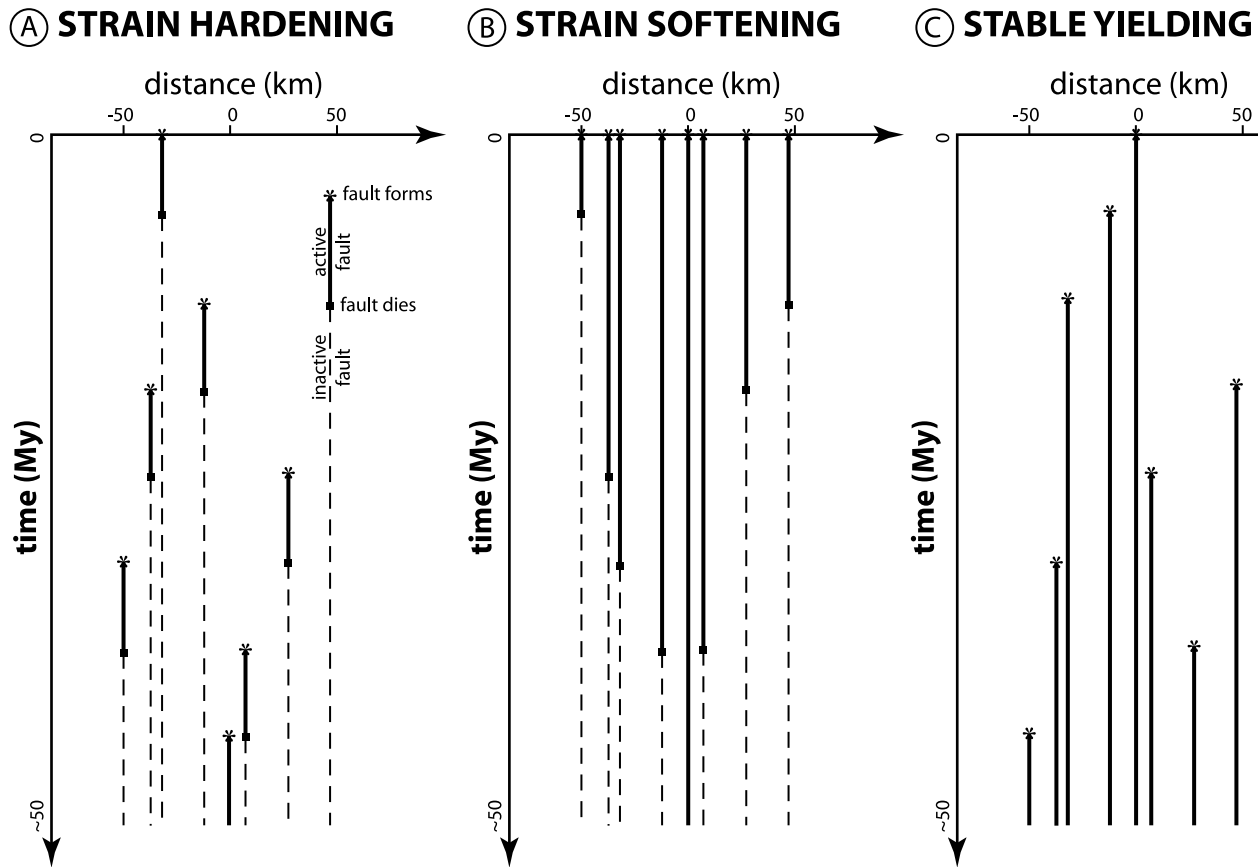


Figure 11. Sketches illustrating different mechanisms for the formation of a broad strike-slip fault system. Horizontal axis show strike-perpendicular width of fault system, vertical axis represents time, increasing downward. (A) Effects of strain-hardening processes on faulting. Fault system forms by the sequential formation and abandonment of individual traces. Only one trace is dominant at any time, and the total width of the fault system increases with time. As we discuss, this pattern of behavior appears to best describe the evolution of the Altyn Tagh fault system. (B) Effects of strain-softening processes. Fault zone initiates as a wide zone of deformation, but slip focuses onto one main trace during progressive deformation. This model predicts that the main trace of the Altyn Tagh fault should be the same age as the fault system as a whole, and is thus inconsistent with the young age of the main trace that we infer. (C) Effects of basal shear. Although the fault system widens with time, here too the main trace and the fault system should be the same age.

implies that the active trace is likewise only a few million years old, even though the Altyn Tagh system has apparently been active since the Middle Eocene or Early Oligocene (Cowgill et al., 2001; Hanson, 1997; Rumelhart, 1998; Yin et al., 2002).

Hardening within the Altyn Tagh System

We speculate that the Altyn Tagh system developed by net strain hardening because the active trace appears to be substantially younger than the 100 km-wide system of subparallel faults in which it is embedded. In particular we suggest that the Altyn Tagh system formed via episodic faulting such as that outlined in Figure 11A: strain first localized within the weakest part of an incipient shear zone to form

a through-going fault, but subsequent hardening resulted in the abandonment of this strand and failure of the next weakest area. This cycle of initial shear localization, strain hardening, fault abandonment, and failure of the next weakest area eventually built a broad system of inactive, subparallel faults that contains a single active trace that is only a few million years old. In the case of the Altyn Tagh system, it appears that individual strands survive for $\sim 5\text{--}10$ m.y., based on the estimated ages for the Akato Tagh bend reported in Cowgill et al. (2004) and the existence of only 3–4 main strands within the ca. 49 Ma Altyn Tagh system (Fig. 1).

Clearly this model predicts that there should be other extinct strike-slip strands within the Altyn Tagh system and that the total displacement on the system will be distributed across

these additional structures. Although more work is needed before these predictions can be fully tested, current understanding of the system supports these predictions. As Figure 1 indicates, several inactive, high-angle Cenozoic faults with either known or inferred left-slip motion lie adjacent to the ATF, and may represent the predicted extinct versions of the Altyn Tagh fault. These structures include the Cherchen and North Altyn faults, as discussed above in the structural framework section. The Kadzi fault cuts Quaternary(?) alluvial deposits and shows left separation of drainages on CORONA imagery near 89°E . Between the Altyn Tagh and Kadzi faults there is a northeast-southwest trending valley that extends from $\sim 87.5^\circ\text{E}$ to $\sim 89.5^\circ\text{E}$, potentially concealing an additional strand within the Altyn Tagh system. The

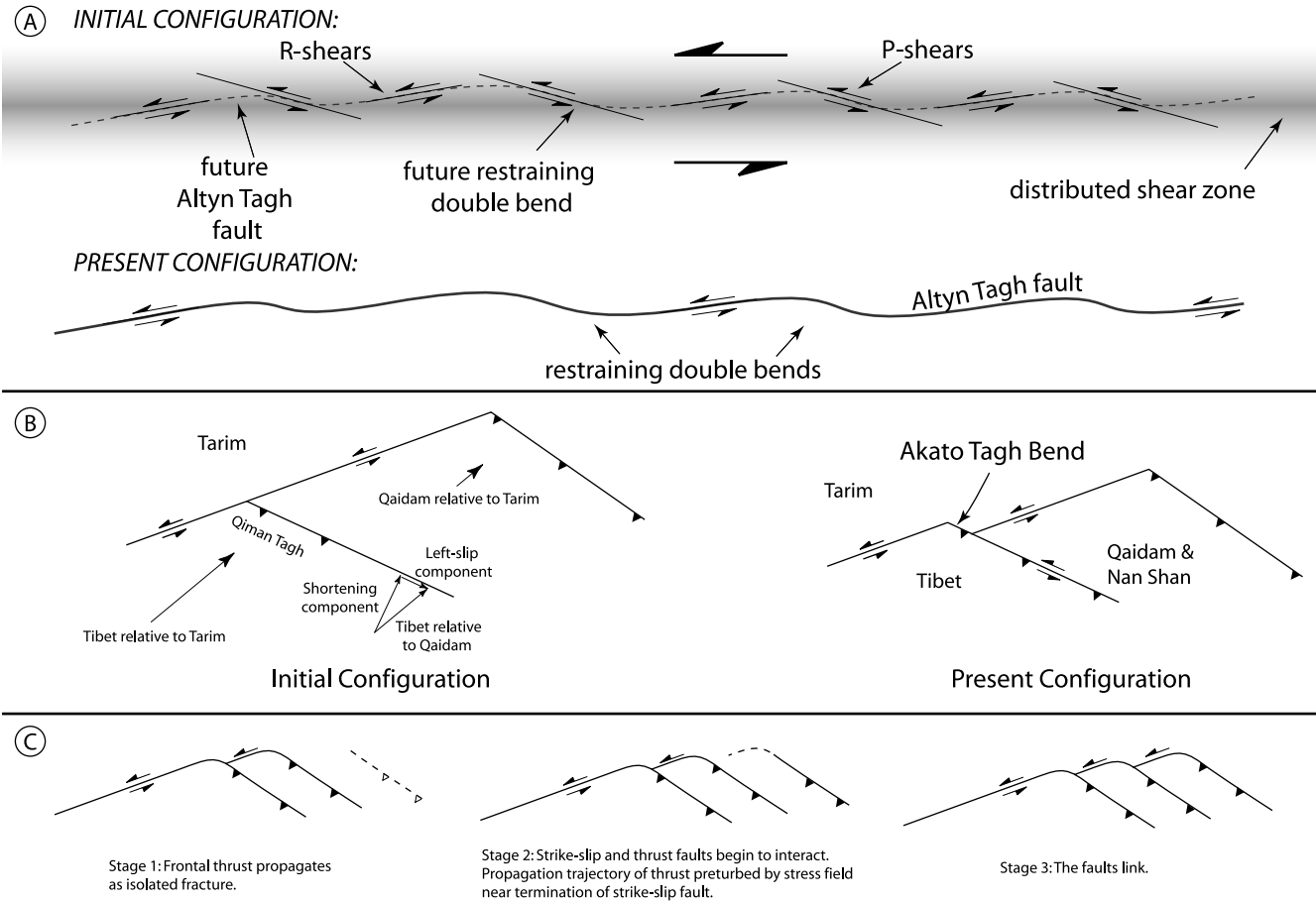


Figure 12. Models for the development of systematic right-stepping bends along the Altyn Tagh fault. (A) Linkage of en echelon R shears by bridging P shears. This model is preferred because it is consistent with the observed slip-directions along the 065°-striking sections of the Altyn Tagh fault. Note that this model allows the main trace to form more recently than the Altyn Tagh system as a whole. (B) Deformation of the fault by relative motion between crustal blocks. Arrows represent transport vectors that permit bend formation. Note that there will be a sinistral component of motion along the Tibet-Qaidam boundary as long as the relative motion vectors for adjacent blocks trend more eastward than the normal to thrust front, but less eastward than the trend of the Altyn Tagh fault. This model is unlikely because it requires transpressional deformation along the western and eastern segments of the Akato Tagh bend, inconsistent with observed pure strike-slip motions reported above. (C) East-directed propagation of the thrust-terminated Altyn Tagh fault. This model is unlikely because it requires that the bends are the same age as the Altyn Tagh system, and thus should be ~50 m.y. old.

internal structure of the Altyn Tagh range between the Altyn Tagh and North Altyn faults is very poorly mapped, except for the area near 90°E (Chen et al., 2003), and additional structures may likewise be present in this region.

Reconstruction of a tectonic boundary across the Altyn Tagh system between 80° and 90°E longitude indicates that total displacement is at least 475 ± 70 km, although accounting for Tibet-Tarim shortening suggests the total is probably ~580 km (Cowgill et al., 2003). Synthesis of recent work permits a very preliminary balancing of the Altyn Tagh system in which the ~580 km total is distributed as ~180 km along the Cherchen fault, ~220 km along the North Altyn strand, and ~180 km along the active

Altyn Tagh fault. We estimate offset along the Cherchen fault by subtracting from the ~580 km total of Cowgill et al. (2003), an estimate of 400 ± 60 km for slip along the Altyn Tagh and North Altyn faults as determined by the reconstruction of a Jurassic facies boundary proposed by Ritts and Biffi (2000). Our suggestion of ~220 km offset along the North Altyn fault is derived by subtracting the 180 km maximum estimate for total slip along the active Altyn Tagh fault derived in Cowgill et al. (2004) from the 400 km North Altyn-Altyn Tagh estimate of Ritts and Biffi (2000). This North Altyn fault slip estimate is probably too high because it does not account for motion along the Kadzi or Keruke faults or any unidentified structures within the Altyn

Tagh range. However, slip along the North Altyn fault should be at least 120 km (Cowgill et al., 2000).

The Race Between Hardening and Softening Processes

Because faults reflect strain localization, it is commonly thought that they are also weak and evolve by strain softening (e.g., Meissner, 1996; Rutter et al., 2001; Sibson, 1977). In contrast, Hobbs et al. (1990) highlighted numerous examples of simultaneous strain localization and hardening. This study also demonstrated the importance of distinguishing the response of the deforming system from that of the deforming

The Race:

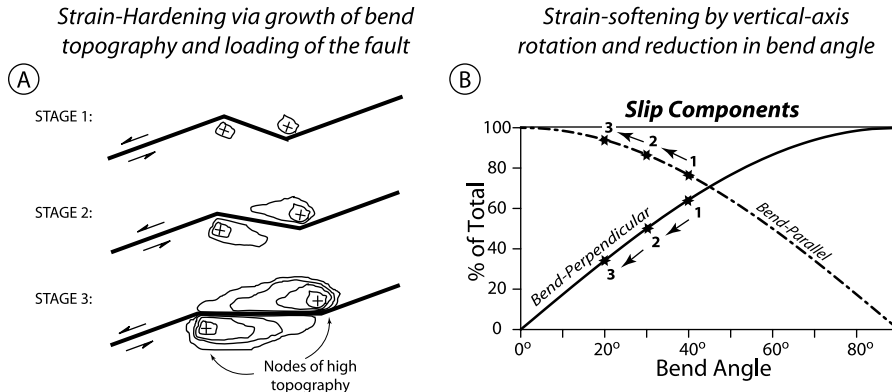


Figure 13. Net strain-hardening or softening of a strike-slip system may reflect a race between hardening via growth of bend topography and loading of the fault and softening via vertical-axis rotation and reduction in bend angle. (A) Evolutionary sequence of a schematic restraining double bend such as the Akato Tagh in which progressive deformation increases topography while also reducing bend angle. Growth of topography by shortening across the bend may perturb the local stress field (i.e., Cowgill et al., 2004) thereby increasing the potential energy of the bend and causing the fault to undergo strain hardening. However, if this shortening is focused in the two inside corners, then the bend should undergo vertical-axis rotation and reduction in bend angle. (B) Plot showing how bend-perpendicular shortening should decrease as bend angle is reduced, thereby producing strain softening. Note that softening by fault rotation as proposed here contrasts with cases of domino-style block rotations that leads to fault abandonment and the formation of multiple, cross-cutting fault sets (e.g., Agnon and Reches, 1995; Nur et al., 1986)

material when considering strain hardening/softening behavior. Specifically, localization can occur in response to boundary conditions during system strain hardening and thus does not always require material strain softening (Hobbs et al., 1990). Likewise, Montési and Zuber (2002) have argued that heterogeneous boundary conditions can produce local stress enhancements and strain localization within materials that do not undergo material softening. We emphasize that the strain-hardening evolution proposed above and in Figure 11A for the Altyn Tagh fault system is a net response of the deforming system that likely reflects a dynamic competition between hardening and softening processes (e.g., Fig. 13).

Several softening processes may have been important within the Altyn Tagh system. For example, linkage of R and P shears to form a through-going fault trace as proposed in Figure 12A should facilitate slip via reduction in fault complexity. Phyllosilicate-rich fault zones such as the Altyn Tagh fault may also undergo softening during the generation of elevated fluid pressures that results from the strongly anisotropic permeability structure of the fault core (e.g., Faulkner et al., 2003; Faulkner and Rutter, 2001). Finally, the vertical-axis rotation of the bend proposed in Cowgill et al. (2004) should

have reduced the bend angle and thus the bend-perpendicular shortening rate (Fig. 13).

These softening mechanisms may have been counterbalanced by two main hardening processes: growth of restraining bend topography (Fig. 13) and material hardening of fault gouge. As Cowgill et al. (2004) suggest, generation of bend topography might produce a switch from thrusting to strike-slip faulting inside the bend in response to the elevated vertical stresses produced by the excess topographic load. Here we further suggest that the growth of topography might increase the gravitational potential energy within the restraining double bend to the point where it becomes easier to break a new fault outside the bend than to continue moving material through it.

Material strain hardening of fault gouge is a second potential strengthening process. In this case, the friction coefficient (μ) of the gouge increases as a function of displacement along the fault. Material hardening is characteristic of experiments on both analog and natural fault gouges, including monomineralic clay gouges (Bird, 1984; Morrow et al., 1992; Morrow et al., 2000; Summers and Byerlee, 1977); crushed granite (Byerlee and Summers, 1976) and quartz (Summers and Byerlee, 1977); samples of natural fault gouge (Morrow

et al., 1982); and mixtures of quartz-montmorillonite (Logan and Rauenzahn, 1987), montmorillonite-illite (Morrow et al., 1992), chrysotile-serpentinite (Moore et al., 1996), and quartz-feldspar (Olsen et al., 1998). Such material hardening may be due to either fabric rotation (Bird, 1984) or fabric formation within the shear zone (Logan and Rauenzahn, 1987; Morrow et al., 1982). In the latter case, initial compaction and grain-size reduction increases contact area and reduces pore volume within the gouge, thereby reducing grain-boundary sliding and increasing grain breakage. This hardening gives way to stable sliding once grain size is reduced to the point where through-going shear fabrics can develop.

Gouges within natural phyllosilicate-rich faults apparently undergo strain hardening similar to their experimental counterparts. For example, the Carboneras fault in Spain appears to have evolved by strain hardening, as suggested by the ~1000 m wide fault core that comprises panels of broken protolith separated by numerous subparallel strands of phyllosilicate gouge (Faulkner et al., 2003). The striking similarity of the Altyn Tagh and Keruke faults (see Cowgill et al., 2004) with the internal structure of the Carboneras fault suggests that these faults may reflect material strain hardening as well.

Bird (1984) noted that the large strains achieved in natural gouges might produce hardening beyond experimentally determined values. Is it possible that natural phyllosilicate gouges might start with the low friction values characteristic of undeformed clay, but strain harden until they are equivalent in strength to their adjacent blocks (i.e., Byerlee's law)? Several studies have reported linear relationships between friction coefficient and shear strain (Morrow et al., 1982) or total displacement (Logan and Rauenzahn, 1987; Moore et al., 1996; Morrow et al., 1992). By extrapolating these relationships, we calculate that only a few tens to a few hundred kilometers of total displacement on a 1000-m-wide fault zone would be required to increase the friction coefficient from a minimum of 0.2 to a maximum of 0.9. This simple analysis assumes that the friction coefficient increases uniformly over the entire displacement interval. Clearly this assumption must be tested before this intriguing mechanism for fault hardening is pursued further.

Implications for Continental Deformation

In summary, we have advanced the idea that geometrically complex strike-slip fault systems such as the Altyn Tagh may form via system strain hardening where this net response reflects a dynamic competition between hardening and

softening processes that are active simultaneously within the fault zone (e.g., Fig. 13). Although clearly speculative, we propose this view because it has the potential to help explain a spectrum of structural styles seen within major continental fault systems and yield insights into the deformational processes at work during their formation. For example, this analysis clearly leads to the suggestion that erosion might strongly impact the first-order geometry of strike slip systems by influencing whether or not such systems evolve by net hardening or softening. More specifically, formation of a new, through-going fault strand via R-P linkage might start a race between softening by vertical axis rotation of the bends, and hardening by growth of bend topography (Fig. 13). High erosion rates should act to suppress hardening by growth of bend topography and may tip the balance in favor of softening processes, causing them to dominate the system response. By contrast, in arid regions like central Asia, erosion rates may be insufficient to hold bend topography in check, thereby driving the system toward net strain hardening.

If the Altyn Tagh fault system has evolved by strain-hardening, and if this process is generally applicable, then it suggests that time scale is critically important in determining whether or not continental deformation is spatially distributed or localized. In particular, this view suggests that in hardening systems, continental deformation is likely to be localized at the short time scales corresponding to the few million years for which any given fault strand will serve as the principal structure. However, the sequential formation, dominance, and death of these discrete structures produces zones of deformation that widen with time. Such progressive widening results in a pattern of continental deformation that is regionally distributed when integrated over the entire life-span of the fault system and the collision zone in which it is contained. Failure to consider the critical role of time scale has been an important oversimplification in the debate over how to best understand continental deformation and can explain why both views seem to be correct.

CONCLUSIONS

The following conclusions can be drawn from our investigation of the active deformation within Akato Tagh restraining double bend.

1. The style of active deformation within the Akato Tagh is highly sensitive to fault orientation. Faults that strike 065°–067° show pure strike-slip motion, whereas faults that strike more northward are transtensional and those that strike more eastward are transpressional.

Sections of the Altyn Tagh fault that lie to the east and west of the Akato Tagh uplift generally strike 065°–070° and are characterized by essentially pure strike-slip motion. Within the double bend the strike of the Altyn Tagh fault changes to 087° and deformation is transpressional. In detail, active structures show a higher degree of correlation between fault orientation and the style of deformation than is evident along the bedrock structures.

2. Active and bedrock structures are generally similar in their geometry and slip directions. In both cases, left-slip predominates along the principal trace of the Altyn Tagh fault, including the EW-striking central segment that defines the Akato Tagh restraining double bend. Deformation is partitioned along this restraining segment, and faults within the adjacent borderlands are dominated by left-slip, rather than thrusting.

3. It remains unclear how bend-perpendicular shortening is actively absorbed along the central segment of the Akato Tagh double bend. However, geomorphic indicators suggest that shortening within the bend is still active: the absence of valley-filling Qm deposits, the concentration of apparently glacially derived Qo fans, and the abundance of steep, narrow channels within the two inside corners of the Akato Tagh uplift suggest these areas may be subjected to faster surface and rock uplift rates than surrounding areas.

4. Based on the observed style of deformation within the Akato Tagh bend and previous studies, we speculate that the importance of northwest-southeast shortening may have been overemphasized along the Altyn Tagh system. It is likely that the main trace of the Altyn Tagh fault is dominated by pure strike-slip motion, because the five straight segments that lie between the four double bends strike roughly parallel to the optimal 065°–070° direction for pure strike-slip motion observed within the Akato Tagh bend. Previous work along the North Altyn fault indicates this structure is dominated by strike-slip motion and not northwest-directed thrusting (Cowgill et al., 2000).

5. It is unlikely that the Akato Tagh double bend has formed by recent deformation of an old trace. Such a process predicts that the western and eastern segments of the bend should be transpressional and not the pure left-slip faults we observed. As a result, it appears that the young age of the Akato Tagh bend probably indicates that the active trace of the Altyn Tagh fault is likewise only a few million years old. We speculate that both the bend and the active trace formed by linkage of an en echelon set of shear fractures during recent development of a new fault strand. The formation of a young strand within a long-lived (ca. 50 Ma) fault system

may indicate that the ~100 km wide Altyn Tagh fault system has formed by net strain-hardening and the sequential formation and death of individual principal traces.

6. Net hardening of geometrically complex strike-slip systems such as the Altyn Tagh may reflect the dominance of strain hardening processes in a dynamic competition between hardening and softening mechanisms that are active simultaneously. In the case of the Altyn Tagh fault we speculate that softening mechanisms may include R-P linkage and reduction in bend angle by vertical-axis rotation, whereas hardening mechanisms could involve growth of bend topography and/or material hardening of phyllosilicate-rich gouge.

7. Fault systems that undergo net strain-hardening may produce patterns of continental deformation that are spatially localized at time scales of 1–5 m.y., but distributed at time scales of 10–100 m.y. Specifically, deformation will be blocklike while any given fault strand serves as the principal structure. However, strain-hardening systems will widen with time as individual, short-lived fault strands sequentially form, become dominant, and then die.

ACKNOWLEDGMENTS

Eric Cowgill thanks Rob Twiss, Todd Ehlers, Paul Kapp, Nadine McQuarrie, Mike Murphy, Zhengkang Shen, and Mike Taylor for their insights and comments on ideas and data presented here. We thank Peter Molnar and Jim Spotila for their thorough reviews. Larry Smith provided access to the GIS laboratory in the Department of Geography at UCLA and Zack Washburn provided instruction in CORONA image rectification. Kristen Ebert digitized the contour lines in Figure 2. We thank Elizabeth Catlos, Jian Anhua, Zhang Shuanhong, the Tarim Petroleum Corporation, and the First Seismological Bureau for their assistance in the field. This project was funded by NSF Continental Dynamics grant EAR9725599.

REFERENCES CITED

- Agnon, A., and Reches, Z., 1995, Frictional rheology: Hardening by rotation of active normal faults: *Tectonophysics*, v. 247, p. 239–254, doi: 10.1016/0040-1951(94)00178-C.
Avouac, J.P., and Tappin, P., 1993, Kinematic model of active deformation in central Asia: *Geophysical Research Letters*, v. 20, no. 10, p. 895–898.
Bally, A.W., Chou, I.M., Clayton, R., Eugster, H.P., Kidwell, S., Meckel, L.D., Ryder, R.T., Watts, A.B., and Wilson, A.A., 1986, Notes on sedimentary basins in China—Report of the American sedimentary basins delegation to the People's Republic of China: U.S. Geological Survey Open File Report 86-327, 108 p.
Bayasgalan, A., Jackson, J., Ritz, J.-F., and Carretier, S., 1999, Field examples of strike-slip fault terminations in Mongolia and their tectonic significance: *Tectonics*, v. 18, no. 3, p. 394–411, doi: 10.1029/1999TC900007.

- Bendick, R., Bilham, R., Freymueller, J., Larson, K., and Yin, G., 2000, Geodetic evidence for a low slip rate in the Altyn Tagh fault system: *Nature*, v. 404, p. 69–72, doi: 10.1038/35003555.
- Bird, P., 1984, Hydration-phase diagrams and friction of montmorillonite under laboratory and geologic conditions, with implications for shale compaction, slope stability, and strength of fault gouge: *Tectonophysics*, v. 107, p. 235–260, doi: 10.1016/0040-1951(84)90253-1.
- Burchfiel, B.C., Deng, Q., Molnar, P., Royden, L., Wang, Y., Zhang, P., and Zhang, W., 1989, Intracrustal detachment zones of continental deformation: *Geology*, v. 17, no. 8, p. 748–752, doi: 10.1130/0091-7613(1989)0172.3.CO;2.
- Byerlee, J., and Summers, R., 1976, A note on the effect of fault gouge thickness on fault stability: *International Journal of Rock Mechanics and Mining Sciences*, v. 13, p. 35–36, doi: 10.1016/0148-9062(76)90226-6.
- Chen, X., Yin, A., Gehrels, G., Cowgill, E., Grove, M., Harrison, T.M., and Wang, X.-F., 2003, Two phases of Mesozoic north-south extension in the eastern Altyn Tagh range, northern Tibetan Plateau: *Tectonics*, v. 22, no. 5, 1053, doi: 10.1029/2001TC001336.
- Chen, Y., Gilder, S., Halim, N., Cogné, J.P., and Courtillot, V., 2002, New paleomagnetic constraints on central Asian kinematics: Displacement along the Altyn Tagh fault and rotation of the Qaidam Basin: *Tectonics*, v. 21, no. 5, 1042, doi: 10.1029/2001TC901030.
- Chen, Z., Burchfiel, B.C., Liu, Y., King, R.W., Royden, L.H., Tang, W., Wang, E., Zhao, J., and Zhang, X., 2000, Global positioning system measurements from eastern Tibet and their implications for India/Eurasia intercontinental deformation: *Journal of Geophysical Research*, v. 105, no. B7, p. 16,215–16,227, doi: 10.1029/2000JB900092.
- Chinese State Bureau of Seismology, 1992, The Altyn Tagh active fault system (in Chinese with English abstract): Beijing, China, Seismology Publishing House, 319 p.
- Cowgill, E., Yin, A., Wang, X.F., and Zhang, Q., 2000, Is the North Altyn fault part of a strike-slip duplex along the Altyn Tagh fault system?: *Geology*, v. 28, no. 3, p. 255–258, doi: 10.1130/0091-7613(2000)0282.3.CO;2.
- Cowgill, E., Yin, A., Harrison, T.M., and Wang, X.-F., 2001, Oligocene initiation of the Central Altyn Tagh fault system inferred from 40Ar/39Ar K-feldspar Thermochronology: *EOS, Transactions, American Geophysical Union*, v. 82, no. 47, p. F1125–F1126.
- Cowgill, E., Yin, A., Harrison, T.M., and Xiao-Feng, W., 2003, Reconstruction of the Altyn Tagh fault based on U-Pb ion microprobe geochronology: Role of back thrusts, mantle sutures, and heterogeneous crustal strength in forming the Tibetan Plateau: *Journal of Geophysical Research*, v. 108, no. B7, 2346, doi: 10.1029/2002JB002080.
- Cowgill, E., Yin, A., Arrowsmith, J.R., Wang, X.-F., and Zhang, S., 2004, The Akato Tagh bend along the Altyn Tagh fault, NW Tibet I, Cenozoic structure, smoothing by vertical-axis rotation, and the effect of topographic stresses on borderland faulting: *Geological Society of America Bulletin*, v. 116, p. 1423–1442, doi: 10.1130/B25359.1.
- Crowell, J.C., 1974, Origin of late Cenozoic basins in southern California, in Dickinson, W.R., ed., *Tectonics and Sedimentation, Society of Economic Paleontologists and Mineralogists*: Tulsa, Oklahoma, Special Publication 22, p. 190–204.
- Cunningham, W.D., Windley, B.F., Dorjnamjaa, D., Badamgarov, J., and Saandar, M., 1996, Late Cenozoic transgression in southwestern Mongolia and the Gobi Altai Tien Shan connection: *Earth and Planetary Science Letters*, v. 140, no. 1–4, p. 67–81, doi: 10.1016/0012-821X(96)00048-9.
- England, P., and Houseman, G., 1986, Finite strain calculations of continental deformation 2, Comparison with the India-Asia collision zone: *Journal of Geophysical Research*, v. 91, no. B3, p. 3664–3676.
- England, P., and Molnar, P., 1997, The field of crustal velocity in Asia calculated from Quaternary rates of slip on faults: *Geophysical Journal International*, v. 130, p. 551–582.
- Faulkner, D.R., and Rutter, E.H., 2001, Can the maintenance of overpressured fluids in large strike-slip fault zones explain their apparent weakness?: *Geology*, v. 29, p. 503–506, doi: 10.1130/0091-7613(2001)0292.0.CO;2.
- Faulkner, D.R., Lewis, A.C., and Rutter, E.H., 2003, On the internal structure and mechanics of large strike-slip fault zones: Field observations of the Carboneras fault in southeastern Spain: *Tectonophysics*, v. 367, p. 235–251, doi: 10.1016/S0040-1951(03)00134-3.
- Friedman, M., Handin, J., Logan, J.M., Min, K.D., and Stearns, D.W., 1976, Experimental folding of rocks under confining pressure: Part III, Faulted drape folds in multilithologic layered specimens: *Geological Society of America Bulletin*, v. 87, p. 1049–1066.
- Hanson, A., 1997, Evidence of Cenozoic erosional unroofing adjacent to the northern Qaidam basin, NW China, preserved within basin margin strata: *Geological Society of America Abstracts with Programs*, v. 29, p. A-143.
- Hobbs, B.E., Mühlhaus, H.-B., and Ord, A., 1990, Instability, softening and localization of deformation, in Knipe, R.J., and Rutter, E.H., eds., *Deformation Mechanisms, Rheology and Tectonics*: London, Geological Society of London Special Publication 54, p. 143–165.
- Holt, W.E., 2000, Correlated crust and mantle strain fields in Tibet: *Geology*, v. 28, p. 67–70, doi: 10.1130/0091-7613(2000)0282.3.CO;2.
- Holt, W.E., Chamot-Rooke, N., Le Pichon, X., Haines, A.J., Shen-Tu, B., and Ren, J., 2000, The velocity field in Asia inferred from Quaternary fault slip rates and Global Positioning System observations: *Journal of Geophysical Research*, v. 105, no. B8, p. 19,185–19,209, doi: 10.1029/2000JB900045.
- Houseman, G.A., and England, P., 1996, A lithospheric-thickening model for the Indo-Asian collision, in Yin, A., and Harrison, T.M., eds., *The Tectonic Evolution of Asia*: New York, Cambridge University Press, p. 3–17.
- Jamison, W.R., 1991, Kinematics of compressional fold development in convergent wrench terranes: *Tectonophysics*, v. 190, p. 209–232, doi: 10.1016/0040-1951(91)90431-Q.
- Jia, C., 1997, *Tectonic Characteristics and Petroleum, Tarim Basin, China*: Beijing, P.R. China, Petroleum Industry Press, 295 p.
- Jolivet, M., Brunel, M., Seward, D., Xu, Z., Yang, J., Roger, F., Tappognier, P., Malavieille, J., Arnaud, N., and Wu, C., 2001, Mesozoic and Cenozoic tectonics of the northern edge of the Tibetan Plateau: fission-track constraints: *Tectonophysics*, p. 111–134.
- Kang, Y., 1996, *Petroleum Geology and Resource Assessment in the Tarim Basin, Xinjiang, China* (in Chinese): Beijing, Geological Publishing House, p. 348.
- Kong, X., and Bird, P., 1996, Neotectonics of Asia: Thin-shell finite-element models with faults, in Yin, A., and Harrison, T.M., eds., *The Tectonic Evolution of Asia*: New York, Cambridge University Press, p. 18–34.
- Lamb, M.A., and Badarch, G., 1997, Paleozoic sedimentary basins and volcanic-arc systems of southern Mongolia: New stratigraphic and sedimentologic constraints: *International Geology Review*, v. 39, p. 542–576.
- Lamb, M.A., Hanson, A.D., Graham, S.A., Badarch, G., and Webb, L.E., 1999, Left-lateral sense offset of Upper Proterozoic to Paleozoic features across the Gobi Onon, Tost, and Zuumbayan faults in southern Mongolia and implications for other central Asian faults: *Earth and Planetary Science Letters*, v. 173, p. 183–194, doi: 10.1016/S0012-821X(99)00227-7.
- Lee, K.Y., 1984, Geology of the Chaidamu basin, Qinghai Province, northwest China: U.S. Geological Survey Open File Report 84-0413, 46 p.
- Liu, Z.Q., 1988, *Geologic Map of the Qinghai-Xizang Plateau and its Neighboring Regions* (in Chinese): Chengdu Institute of Geology and Mineral Resources, Academica Sinica Geology Publisher, scale 1:1,500,000.
- Logan, J.M., and Rauenzahn, K.A., 1987, Frictional dependence of gouge mixtures of quartz and montmorillonite on velocity, composition and fabric: *Tectonophysics*, v. 144, p. 87–108, doi: 10.1016/0040-1951(87)90010-2.
- Ma, X., 1980, *Lithospheric Dynamics Map of China and Adjacent Seas*: Beijing, China, Geological Publishing House.
- Meissner, R., 1996, Faults and folds, fact and fiction: *Tectonophysics*, v. 264, p. 279–293, doi: 10.1016/S0040-1951(96)00132-1.
- Meriaux, A., Tapponnier, P., Ryerson, F.J., Van der Woerd, J., King, G., Meyer, B., Finkel, R., and Caffee, M., 1997, Application of cosmogenic ^{10}Be and ^{26}Al dating to neotectonics of the Altyn Tagh fault in central Asia (Gansu, China): *EOS, Transactions, American Geophysical Union*, v. 78, no. 46, p. F173.
- Meriaux, A.S., Ryerson, F.J., Tapponnier, P., Van der Woerd, J., Lasserre, C., and Xu, X., 1998, Large-scale strain patterns, great earthquakes, and Late Pleistocene slip-rate along the Altyn Tagh fault (China): *EOS, Transactions, American Geophysical Union*, v. 79, no. 45, p. F190.
- Meriaux, A.-S., Ryerson, F.J., Tapponnier, P., Van der Woerd, J., Finkel, R.C., Caffee, M.W., Lasserre, C., Xu, X., Li, H., and Xu, Z., 2000, Fast extrusion of the Tibet Plateau: A 3 cm/yr, 100 Kyr slip-rate on the Altyn Tagh fault: *EOS, Transactions, American Geophysical Union*, v. 81, no. 48, p. F1137.
- Meyer, B., Tapponnier, P., Gaudemer, Y., Peltzer, G., Guo, S., and Chen, Z., 1996, Rate of left-lateral movement along the easternmost segment of the Altyn Tagh fault, east of 96°E (China): *Geophysical Journal International*, v. 124, p. 29–44.
- Meyer, B., Tapponnier, P., Bourjot, L., Metivier, F., Gaudemer, Y., Peltzer, G., Guo, S., and Chen, Z., 1998, Crustal thickening in Gansu-Qinghai, lithospheric mantle subduction, and oblique, strike-slip controlled growth of the Tibet plateau: *Geophysical Journal International*, v. 135, p. 1–47, doi: 10.1046/J.1365-246X.1998.00567.X.
- Miller, D.D., 1998, Distributed shear, rotation, and partitioned strain along the San Andreas fault, central California: *Geology*, v. 26, p. 867–870, doi: 10.1130/0091-7613(1998)0262.3.CO;2.
- Molnar, P., and Tapponnier, P., 1975, Cenozoic tectonics of Asia: effects of a continental collision: *Science*, v. 189, no. 4201, p. 419–426.
- Molnar, P., and Tapponnier, P., 1978, Active tectonics of Tibet: *Journal of Geophysical Research*, v. 83, no. B11, p. 5361–5375.
- Molnar, P., Burchfiel, B.C., Kuangyi, L., and Ziyun, Z., 1987a, Geomorphic evidence for active faulting in the Altyn Tagh and northern Tibet and qualitative estimates of its contribution to the convergence of India and Eurasia: *Geology*, v. 15, p. 249–253.
- Molnar, P., Burchfiel, B.C., Zhao, Z., Liang, K., Wang, S., and Huang, M., 1987b, Geologic evolution of northern Tibet: Results of an expedition to Ulugh Muztagh: *Science*, v. 235, p. 299–305.
- Montési, L.G.J., and Zuber, M.T., 2002, A unified description of localization for application to large-scale tectonics: *Journal of Geophysical Research*, v. 107, no. B3, p. 2045, doi: 10.1029/2001JB000465.
- Moore, D.E., Lockner, D.A., Summers, R., Ma, S., and Byerlee, J.D., 1996, Strength of chrysotile-serpentinite gouge under hydrothermal conditions: Can it explain a weak San Andreas fault?: *Geology*, v. 24, no. 11, p. 1041–1044, doi: 10.1130/0091-7613(1996)0242.3.CO;2.
- Morrow, C.A., Shi, L.Q., and Byerlee, J.D., 1982, Strain hardening and strength of clay-rich fault gouges: *Journal of Geophysical Research*, v. 87, no. B8, p. 6771–6780.
- Morrow, C.A., Radney, B., and Byerlee, J., 1992, Frictional strength and the effective pressure law of montmorillonite and illite clays, in Evans, B., and Wong, T.-f., eds., *Fault Mechanics and Transport Properties of Rocks*: London, Academic Press Ltd., p. 69–88.
- Morrow, C.A., Moore, D.E., and Lockner, D.A., 2000, The effect of mineral bond strength and adsorbed water on fault gouge frictional strength: *Geophysical Research Letters*, v. 27, no. 6, p. 815–818, doi: 10.1029/1999GL008401.
- Nur, A., Ron, H., and Scotti, O., 1986, Fault mechanics and the kinematics of block rotations: *Geology*, v. 14, p. 746–749.
- Olsen, M.P., Scholz, C.H., and Léger, A., 1998, Healing and sealing of a simplified fault gouge under hydrothermal conditions: Implications for fault healing: *Journal of Geophysical Research*, v. 103, no. B4, p. 7421–7430, doi: 10.1029/97JB03402.
- Owen, L.A., and Derbyshire, E., 1988, Glacially deformed diamictites in the Karakorum Mountains, Northern

- Pakistan, in Croot, D., ed., *Glaciodynamics: Forms and Processes*: Rotterdam, Balkema, p. 149–176.
- Peltzer, G., and Saucier, F., 1996, Present-day kinematics of Asia derived from geologic fault rates: *Journal of Geophysical Research*, v. 101, no. B12, p. 27,943–27,956, doi: 10.1029/96JB02698.
- Peltzer, G., and Tapponniere, P., 1988, Formation and evolution of strike-slip faults, rifts, and basins during the India-Asia collision: An experimental approach: *Journal of Geophysical Research*, v. 93, no. B12, p. 15,085–15,117.
- Philip, H., Rogozhin, E., Cisternas, A., Bousquet, J.C., Borisov, B., and Karakhanian, A., 1992, The Armenian earthquake of 1988 December 7: Faulting and folding, neotectonics and paleoseismicity: *Geophysical Journal International*, v. 110, p. 141–158.
- Ritts, B.D., and Biffi, U., 2000, Magnitude of post-Middle Jurassic (Bajocian) displacement on the Altyn Tagh fault system, northwest China: *Geological Society of America Bulletin*, v. 112, p. 61–74, doi: 10.1130/0016-7606(2000)112.3.CO;2.
- Robinson, D., Dupont-Nivet, G., Gehrels, G.E., and Zhang, Y., 2003, The Tula uplift, northwestern China: Evidence for regional tectonism of the northern Tibetan Plateau during late Mesozoic-early Cenozoic time: *Geological Society of America Bulletin*, v. 115, p. 35–47, doi: 10.1130/0016-7606(2003)1152.0.CO;2.
- Roy, M., and Royden, L.H., 2000a, Crustal rheology and faulting at strike-slip plate boundaries; 1, An analytic model: *Journal of Geophysical Research*, v. 105, no. B3, p. 5583–5597, doi: 10.1029/1999JB900339.
- Roy, M., and Royden, L.H., 2000b, Crustal rheology and faulting at strike-slip plate boundaries; 2, Effects of lower crustal flow: *Journal of Geophysical Research*, v. 105, no. B3, p. 5599–5613, doi: 10.1029/1999JB900340.
- Rumelhart, P.E., 1998, Cenozoic basin evolution of southern Tarim, northwestern China: Implications for the uplift history of the Tibetan Plateau [Ph.D. thesis]: Los Angeles, University of California, 268 p.
- Rumelhart, P., Yin, A., Cowgill, E., Butler, R., Zhang, Q., and Wang, X.F., 1999, Cenozoic vertical-axis rotation of the Altyn Tagh fault system: *Geology*, v. 27, p. 819–822, doi: 10.1130/0091-7613(1999)027.3.CO;2.
- Rutter, E.H., Holdsworth, R.E., and Knipe, R.J., 2001, The nature and tectonic significance of fault-zone weakening: An introduction, in Holdsworth, R.E., Strachan, R.A., Magloughlin, J.F., and Knipe, R.J., eds., *The Nature and Tectonic Significance of Fault Zone Weakening*: London, Geological Society of London Special Publication 186, p. 1–11.
- Shen, Z.-K., Wang, M., Li, Y., Jackson, D.D., Yin, A., Dong, D., and Fang, P., 2001, Crustal deformation along the Altyn Tagh fault system, western China, from GPS: *Journal of Geophysical Research*, v. 106, no. B12, p. 30,607–30,621, doi: 10.1029/2001JB000349.
- Sibson, R.H., 1977, Fault rocks and fault mechanisms: *Journal of the Geological Society of London*, v. 133, p. 191–213.
- Sobel, E.R., Arnaud, N., Jolivet, M., Ritts, B.D., and Brunel, M., 2001, Jurassic to Cenozoic exhumation history of the Altyn Tagh range, northwest China, constrained by $^{40}\text{Ar}/^{39}\text{Ar}$ and apatite fission track thermochronology, in Hendrix, M.S., and Davis, G.A., eds., *Paleozoic and Mesozoic Tectonic Evolution of Central and Eastern Asia: From Continental Assembly to Intracontinental Deformation*: Boulder, Colorado, Geological Society of America Memoir 194, p. 247–267.
- Song, T., and Wang, X., 1993, Structural styles and stratigraphic patterns of syndepositional faults in a contractional setting: Examples from Quaidam basin, northwestern China: *AAPG Bulletin*, v. 77, no. 1, p. 102–117.
- Summers, R., and Byerlee, J., 1977, A note on the effect of fault gouge composition on the stability of frictional sliding: *International Journal of Rock Mechanics and Mining Sciences*, v. 14, p. 155–160, doi: 10.1016/0148-9062(77)90007-9.
- Tapponniere, P., and Molnar, P., 1977, Active faulting and tectonics in China: *Journal of Geophysical Research*, v. 82, no. 20, p. 2905–2930.
- Tapponniere, P., Meyer, B., Avouac, J.P., Peltzer, G., Gaudemer, Y., Guo, S., Xiang, H., Yin, K., Chen, Z., Cai, S., and Dai, H., 1990, Active thrusting and folding in the Qilian Shan and decoupling between upper crust and mantle in northeastern Tibet: *Earth and Planetary Science Letters*, v. 97, p. 382–403, doi: 10.1016/0012-821X(90)90053-Z.
- Tapponniere, P., Xu, Z., Roger, F., Meyer, B., Arnaud, N., Wittlinger, G., and Yang, J., 2001, Oblique stepwise rise and growth of the Tibet Plateau: *Science*, v. 294, no. 5547, p. 1671–1677, doi: 10.1126/SCIENCE.105978.
- Tchalenko, J.S., 1970, Similarities between shear zones of different magnitudes: *Geological Society of America Bulletin*, v. 81, p. 1625–1640.
- Teyssier, C., and Tikoff, B., 1998, Strike-slip partitioned transpression of the San Andreas fault system: A lithospheric-scale approach, in Holdsworth, R.E., Strachan, R.A., and Dewey, J.F., eds., *Continental Transpressional and Transtensional Tectonics*: London, Geological Society, p. 143–158.
- Van der Woerd, J., Ryerson, F.J., Tapponniere, P., Gaudemer, Y., Finkel, R., Meriaux, A.S., Caffee, M., Zhao, G., and He, Q., 1998, Holocene left-slip rate determined by cosmogenic surface dating on the Xidatan segment of the Kunlun fault (Qinghai, China): *Geology*, v. 26, p. 695–698, doi: 10.1130/0091-7613(1998)026.3.CO;2.
- Van der Woerd, J., Xu, X., Li, H., Tapponniere, P., Meyer, B., Ryerson, F.J., Meriaux, A.-S., and Xu, Z., 2001, Rapid active thrusting along the northwestern rangefront of the Tanghe Nan Shan (western Gansu, China): *Journal of Geophysical Research*, v. 106, no. B12, p. 30,475–30,504, doi: 10.1029/2001JB000583.
- Van der Woerd, J., Tapponniere, P., Ryerson, F.J., Meriaux, A.-S., Meyer, B., Gaudemer, Y., Finkel, R.C., Caffee, M.W., Zhao, G., and Xu, Z., 2002, Uniform postglacial slip-rate along the central 600 km of the Kunlun fault (Tibet), from ^{26}Al , ^{10}Be and ^{14}C dating of riser offsets, and climatic origin of the regional morphology: *Geophysical Journal International*, v. 148, p. 356–388, doi: 10.1046/J.1365-246X.2002.01556.X.
- Wang, E., 1997, Displacement and timing along the northern strand of the Altyn Tagh fault zone, Northern Tibet: *Earth and Planetary Science Letters*, v. 150, p. 55–64, doi: 10.1016/S0012-821X(97)00085-X.
- Washburn, Z., 2001, Quaternary tectonics and earthquake geology of the central Altyn Tagh fault, Xinjiang, China: Implications for tectonic processes along the northern margin of Tibet [M.S. thesis]: Tempe, Arizona State University, 179 p.
- Washburn, Z., Arrowsmith, J.R., Dupont-Nivet, G., and Wang, X.-F., 2000, Earthquake geology of the Central Altyn Tagh fault from Lake Wuzhunxiao (38.4N, 89.9E) to Lapequan (39.1N, 92.5E), China: *EOS*, Transactions, American Geophysical Union, v. 81, no. 48, p. F1137.
- Washburn, Z., Arrowsmith, J.R., Forman, S.L., Cowgill, E., Wang, X., Zhang, Y., and Chen, Z., 2001, Late Holocene earthquake history of the central Altyn Tagh Fault, China: *Geology*, v. 29, no. 11, p. 1051–1054, doi: 10.1130/0091-7613(2001)029.2.CO;2.
- Washburn, Z., Arrowsmith, J.R., DuPont-Nivet, G., Wang, X.-F., Zhang, Y.-Q., and Chen, Z., 2003, Earthquake geology of the central Altyn Tagh Fault, Xinjiang, China: *Annals of Geophysics*, v. 46, no. 5, p. 1015–1034.
- Wessel, P., and Smith, W.H.F., 1991, Free software helps map and display data: *EOS, Transactions, American Geophysical Union*, v. 72, p. 441.
- Wittlinger, G., Tapponniere, P., Poupinet, G., Jiang, M., Shi, D., Herquel, G., and Masson, F., 1998, Tomographic evidence for localized lithospheric shear along the Altyn Tagh fault: *Science*, v. 282, p. 74–76, doi: 10.1126/SCIENCE.282.5386.74.
- Xinjiang Bureau of Geology and Mineral Resources, 1993, *Regional Geology of Xinjiang Uygur Autonomous Region* (in Chinese with English abstract), Geological Memoirs of the Ministry of Geology and Mineral Resources: Beijing, P.R. China, Geological Publishing House, 841 p.
- Yin, A., and Harrison, T.M., 2000, Geologic evolution of the Himalayan-Tibetan orogen: *Annual Review of Earth and Planetary Science*, v. 28, p. 211–280, doi: 10.1146/ANNUREV.EARTH.28.1.211.
- Yin, A., and Nie, S., 1996, A Phanerozoic palinspastic reconstruction of China and its neighboring regions, in Yin, A., and Harrison, T.M., eds., *The Tectonic Evolution of Asia*: New York, Cambridge University Press, p. 442–485.
- Yin, A., Yang, Z., Butler, R., Otofuji, Y.-I., Rumelhart, P.E., and Cowgill, E., 2000, Correction: Cenozoic vertical-axis rotation of the Altyn Tagh fault system: *Geology*, v. 28, no. 5, p. 480.
- Yin, A., Rumelhart, P.E., Butler, R., Cowgill, E., Harrison, T.M., Foster, D.A., Ingersoll, R.V., Zhang, Q., Zhou, X.-Q., Wang, X.-F., Hanson, A., and Raza, A., 2002, Tectonic history of the Altyn Tagh fault system in northern Tibet inferred from Cenozoic sedimentation: *Geological Society of America Bulletin*, v. 114, no. 10, p. 1257–1295, doi: 10.1130/0016-7606(2002)114.10.CO;2.
- Yue, Y., Ritts, B.D., and Graham, S.A., 2001, Initiation and long-term slip history of the Altyn Tagh fault: *International Geology Review*, v. 43, no. 2001, p. 1087–1093.
- Yue, Y., Ritts, B.D., Graham, S.A., Wooden, J.L., Gehrels, G.E., and Zhang, Z., 2003, Slowing extrusion tectonics: Lowered estimate of post-Early Miocene slip rate for the Altyn Tagh fault: *Earth and Planetary Science Letters*, v. 217, p. 111–122, doi: 10.1016/S0012-821X(03)00544-2.
- Zheng, J., 1991, Significance of the Altyn Tagh fault of China: *Episodes*, v. 14, no. 4, p. 307–312.
- Zheng, J., 1994, *Geodynamics of Altyn Tagh Fault*: Journal of China University of Geosciences, v. 5, no. 1, p. 41–45.

MANUSCRIPT RECEIVED BY THE SOCIETY 21 MARCH 2003

REVISED MANUSCRIPT RECEIVED 29 DECEMBER 2003

MANUSCRIPT ACCEPTED 28 JANUARY 2004

Printed in the USA

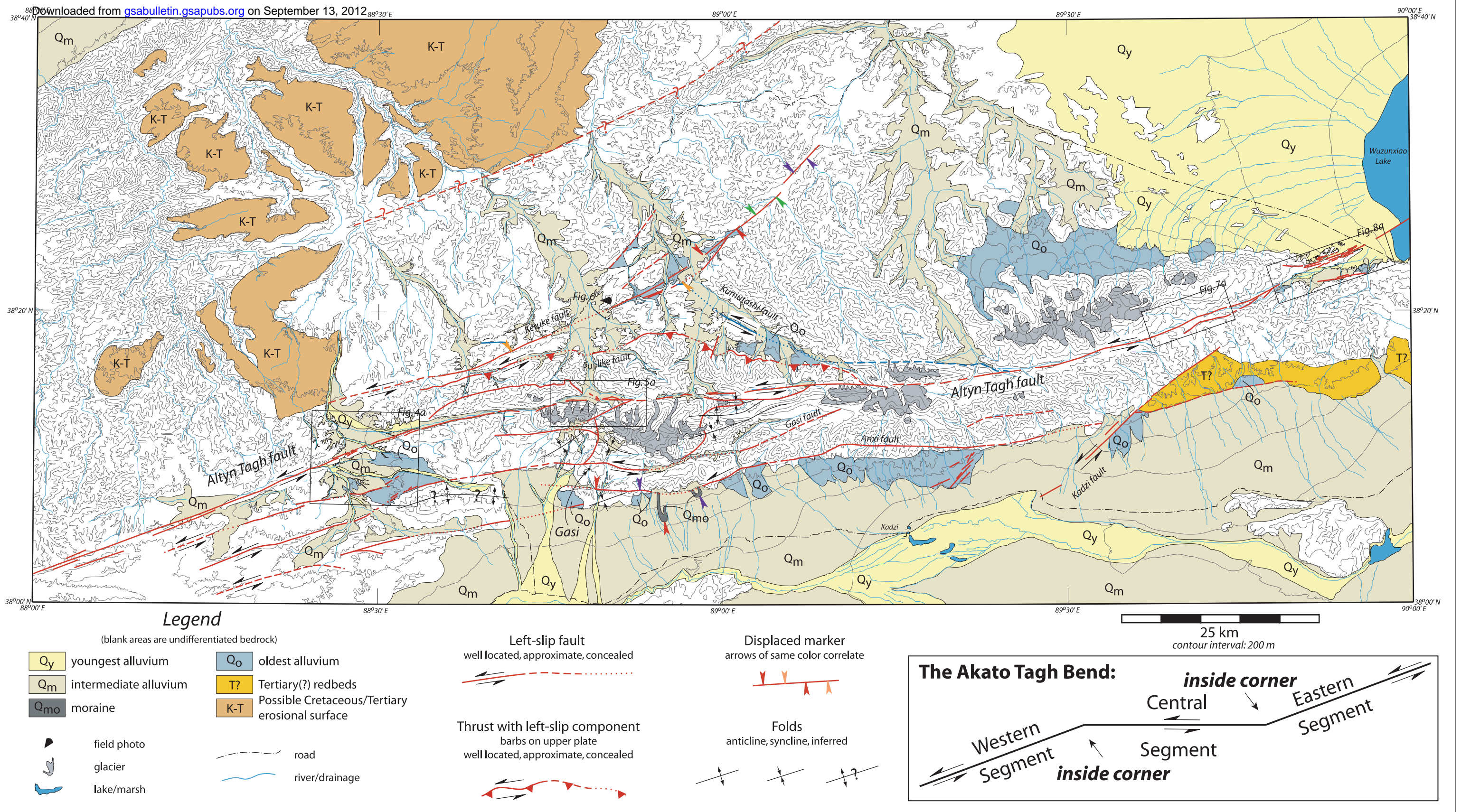


Figure 2. Fault map of the Akato Tagh double bend showing recent and active structures, associated glaciated peaks, and the distribution of old (Q_o), intermediate (Q_m), and young (Q_y) Quaternary deposits. Also shown are locations of an apparent low-relief erosion surface (relict landscape) of possible late Mesozoic to early Cenozoic age, and exposures of Tertiary(?) redbeds. Unlabeled portions of the map are older than Cretaceous. Quaternary units and faults were compiled from our mapping and CORONA image analysis, as well as the active fault map of the Altyn Tagh fault (Chinese State Bureau of Seismology, 1992). Inset shows the locations of the western, central, and eastern segments of the Akato Tagh bend and the positions of the two inside corners. Note that the highest topography in the area is concentrated within these two corners (also see Cowgill et al., 2004). Offset markers are indicated by pairs of arrows with matching colors. Boxes outline areas where we have mapped the active deformation. Topographic base with 200 m contour interval was simplified from 1:100,000 topographic maps.

The Akato Tagh bend along the Altyn Tagh fault, northwest Tibet 2: Active deformation and the importance of transpression and strain hardening within the Altyn Tagh system

Eric Cowgill, J Ramón Arrowsmith, An Yin, Wang Xiaofeng, and Chen Zhengle
Figure 2: Supplement to: *Geological Society of America Bulletin*, v. 116, no. 11/12

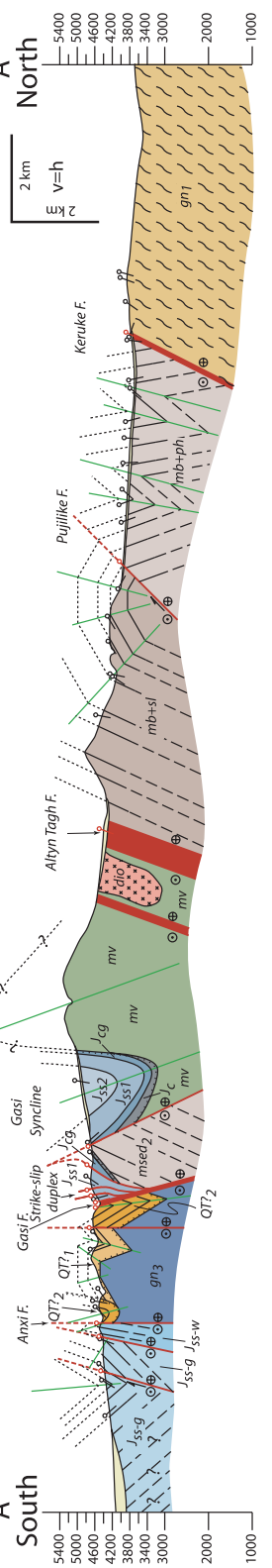
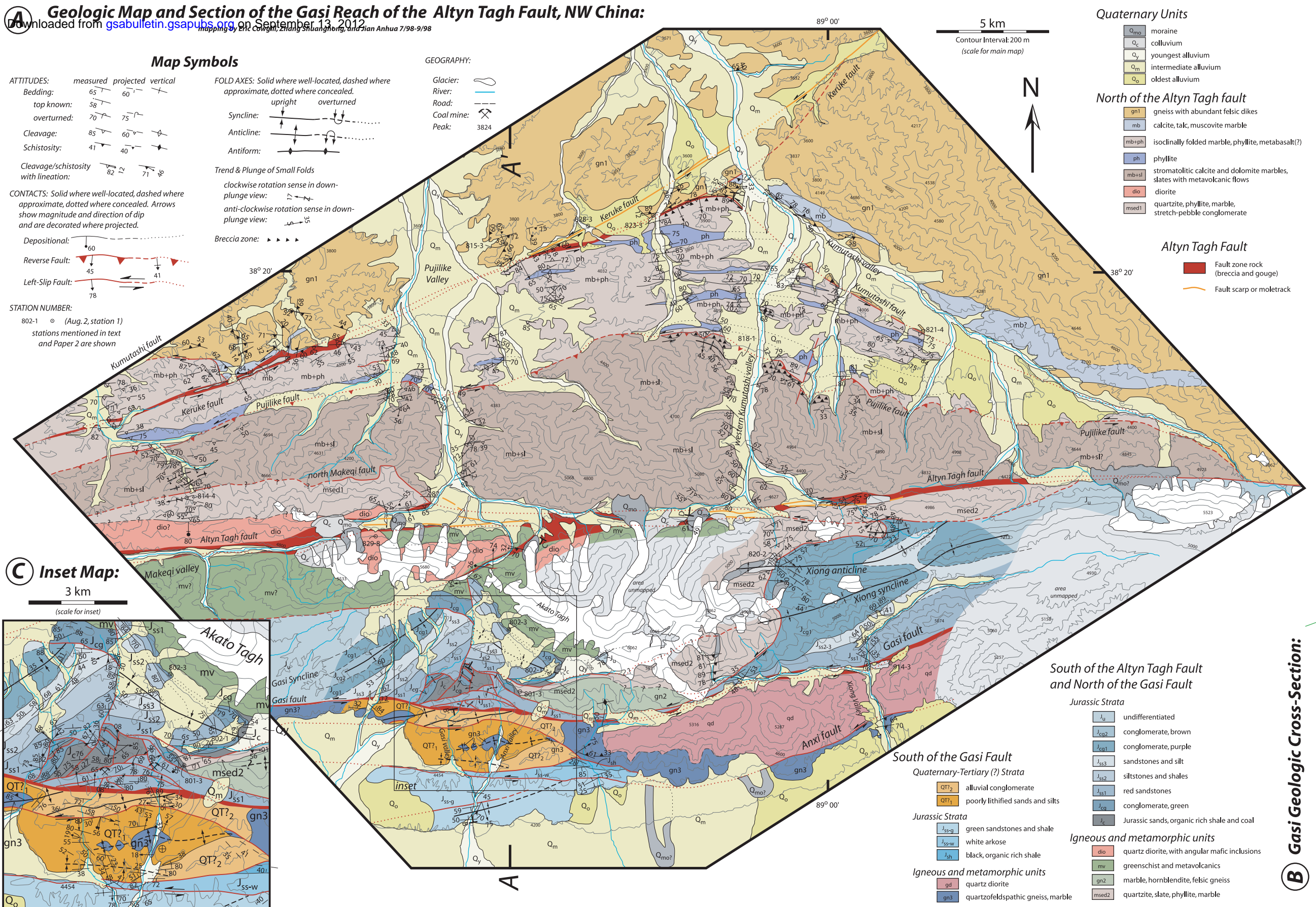


Figure 4. Geology of the western half of the Akato Tagh bend. (A) Geologic map of the Gasi area based on 1:100,000 scale field mapping. Strike-slip faults predominate in the southern strike-slip borderlands and include a fault that has been folded by the Xiong anticline and syncline. Stations 829-8 and 914-3 show the location of samples 98-8-29-8a and 98-9-14-3a, respectively, for which U-Pb zircon analyses are reported in Cowgill et al. (2003). (B) Geologic section along line A-A'. (C) Detailed map showing structural complexity in the vicinity of the Gasi and Anxi coal mines.

The Akato Tagh bend along the Altyn Tagh fault, northwest Tibet 1: Smoothing by vertical-axis rotation and the effect of topographic stresses on bend-flanking faults
Eric Cowgill, An Yin, J Ramón Arrowsmith, Wang Xiao Feng, and Zhang Shuanhong
Figure 4: Supplement to: *Geological Society of America Bulletin*, v. 116, no. 11/12